CellPress

Cell Host & Microbe
Short Article

Host Cell Phosphatidylcholine Is a Key Mediator of Malaria Parasite Survival during Liver Stage Infection

Maurice A. Itoe,[1] Júlio L. Sampaio,[2] Ghislain G. Cabal,[1] Eliana Real,[1] Vanessa Zuzarte-Luis,[1] Sandra March,[3] Sangeeta N. Bhatia,[3] Friedrich Frischknecht,[4] Christoph Thiele,[5] Andrej Shevchenko,[2] and Maria M. Mota[1,*]
[1]Instituto de Medicina Molecular, Faculdade de Medicina da Universidade de Lisboa, 1649-028 Lisboa, Portugal
[2]Max Planck Institute of Molecular cell Biology and Genetics, 01307 Dresden, Germany
[3]Institute for Medical Engineering and Science/Koch Institute, Massachusetts Institute of Technology, Cambridge, MA 02139, USA
[4]Department of Infectious Diseases, University of Heidelberg Medical School, 69120 Heidelberg, Germany
[5]Laboratory of Biochemistry and Cell Biology of Lipids, Life and Medical Sciences Institute, University of Bonn, 53115 Bonn, Germany
*Correspondence: mmota@medicina.ulisboa.pt
http://dx.doi.org/10.1016/j.chom.2014.11.006

SUMMARY

During invasion, *Plasmodium*, the causative agent of malaria, wraps itself in a parasitophorous vacuole membrane (PVM), which constitutes a critical interface between the parasite and its host cell. Within hepatocytes, each *Plasmodium* sporozoite generates thousands of new parasites, creating high demand for lipids to support this replication and enlarge the PVM. Here, a global analysis of the total lipid repertoire of *Plasmodium*-infected hepatocytes reveals an enrichment of neutral lipids and the major membrane phospholipid, phosphatidylcholine (PC). While infection is unaffected in mice deficient in key enzymes involved in neutral lipid synthesis and lipolysis, ablation of rate-limiting enzymes in hepatic PC biosynthetic pathways significantly decreases parasite numbers. Host PC is taken up by both *P. berghei* and *P. falciparum* and is necessary for correct localization of parasite proteins to the PVM, which is essential for parasite survival. Thus, *Plasmodium* relies on the abundance of these lipids within hepatocytes to support infection.

INTRODUCTION

Lipids play key roles in many biological processes; ranging from a structural role in membranes to signaling, in addition to being sources of metabolic energy (Bohdanowicz and Grinstein 2013; van Meer and Sprong 2004; van Meer et al., 2008).

Malaria infection is initiated when *Plasmodium* sporozoites enter the mammalian host through the bite of an infected female *Anopheles* mosquito. During a blood meal, ~10–100 sporozoites are deposited under the skin of the host and travel to the liver, where they infect hepatocytes. Each sporozoite resides in a hepatocyte for 2–14 days (2 days for *P. berghei* and ~7 days for *P. falciparum*), multiplying into >10,000 merozoites, which are then released in the bloodstream to infect red blood cells, initiating the symptoms of malaria (Prudêncio et al., 2006). The rapid replication of *Plasmodium* parasites in hepatocytes requires important lipid resources to support organelle and membrane neogenesis, the growth of the parasitophorous vacuole membrane (PVM), and possibly the maintenance of host cell and parasite homeostasis and survival (Prudêncio et al., 2006). Such demand is likely to be satisfied by import of hepatocyte lipids, as well as by de novo synthesis by the apicoplast fatty acid synthesis II (FAS II) system (Ralph et al., 2004) and the plethora of parasite-encoded phospholipid biosynthetic enzymes (Déchamps et al., 2010).

Transcriptomic studies revealed that the apicoplast-resident enzymes involved in the FAS II system are upregulated throughout liver stage infection (Tarun et al., 2008). While these and other enzymes of the pyruvate dehydrogenase complex are critical for the formation of infective merozoites, parasites lacking these enzymes initiate replication in the liver normally (Pei et al., 2010; Vaughan et al., 2009; Yu et al., 2008). Likewise, parasites deficient in octanoyl-ACP transferase or lipoic acid protein ligase (LipB), a limiting enzyme in the derivation of lipoic acid from a major FAS II product, octanoyl-ACP, show a similar phenotype. In addition, *P. yoelii* parasites deficient in glycerol-3-phosphate dehydrogenase and glycerol-3-phosphate acyltransferase, key enzymes in the synthesis of the phospholipid precursor phosphatidic acid, develop normally, but again do not form merozoites (Lindner et al., 2014). These data imply that, despite the ability to synthesize fatty acids de novo, *Plasmodium* depends on host lipids during part or the entire pre-erythrocytic cycle.

Our previous work revealed that host genes involved in lipid metabolism are transcriptionally modulated during *Plasmodium* intrahepatic development (Albuquerque et al., 2009). Also, scavenger receptor binding protein 1, a membrane protein important for cellular cholesterol homeostasis, is key for in vitro infection (Rodrigues et al., 2008; Yalaoui et al., 2008). *Plasmodium* parasites scavenge cholesterol from the host irrespective of whether it has been internalized via the LDL receptor or synthesized de novo. Inhibition of either source of host cholesterol decreased the cholesterol content in merozoites but did not have any effect on liver stage development. On the other hand, scavenging of

lipoic acid from the host cell into parasite mitochondria was shown to be critical for *P. berghei* survival in hepatocytes (Allary et al., 2007; Deschermeier et al., 2012). Despite these advances, the contribution of host cell lipid metabolic pathway(s) to the establishment of a successful infection in hepatocytes is largely unexplored.

Aiming at understanding the dynamics of lipids during *Plasmodium* liver stage infection, we performed shotgun mass spectrometry analysis of the total cellular lipidome in *P. berghei*-infected versus noninfected cells at different points throughout infection. These analyses revealed major alterations in lipids involved in storage and membrane biogenesis, including phosphatidylcholine (PC), one of the major membrane phospholipids. Combining targeted silencing of host genes involved in de novo PC synthesis with visualization of host PC, we show that *Plasmodium* uptakes host-derived PC and that the activity of the two host de novo PC synthesis pathways is critical for the establishment of *Plasmodium* in the mammalian liver.

RESULTS

Lipid Composition of *P. berghei*-Infected Hepatocytes Is Altered during Infection

To assess whether changes in gene expression of major lipid biosynthetic pathways in the host and the parasite transcriptomes (Albuquerque et al., 2009; Tarun et al., 2008) correlated with changes in the total lipidome of hepatocytes upon infection with *Plasmodium* sporozoites, we performed quantitative Shotgun Lipidomics experiments on *P. berghei*-infected and noninfected Huh7 hepatoma cells (Figure 1A). Initial mass spectrometry analysis of noninfected Huh7 cells showed that the amount of lipids extracted was proportional to the number of cells used and that the minimal number of cells necessary to detect major lipid classes was 10^4 cells (Figure S1 available online). Due to the low infectivity of *Plasmodium* sporozoites, we isolated GFP-expressing *P. berghei*-infected and noninfected cells by fluorescence-activated cell sorting (FACS) (Prudêncio et al., 2008) at 25, 35, and 45 hr (h) after infection, which are representative time points of early parasite replication, liver schizogony, and the early cellularization process leading to the formation of individual merozoites. The number of cells used in this study ranged from 4.5 to 30 × 10^4 per sample. The relative abundance or total abundance of each lipid class was expressed as molar percentage of total lipidome or normalized as the total lipid per number of cells at any given time, respectively (Figure S1).

Major and significant alterations in the lipidome of *P. berghei*-infected cells were observed (see Table S1 for entire raw data). The neutral lipids triacylglycerol (TAG), diacylglycerol (DAG), and cholesterol esters (CEs) were increased at 25 hr after infection; however, at later time points their levels had subsided to those of control cells (Figures 1B and S1). Additionally, an enrichment of PC, the main structural membrane phospholipid, was observed in infected cells throughout infection, concomitant with a persistent and significant decrease in the levels of all anionic phospholipids: phosphatidylethanolamine (PE), phosphatidylserine (PS), phosphatidic acid (PA), and phosphatidylinositol (PI) (Figure 1B). Altogether, the lipidomic data suggest that key aspects of hepatic lipid metabolism such as lipogenesis/lipolysis, in addition to phospholipid headgroup remodeling pathways, are actively engaged during *Plasmodium* infection of hepatocytes.

Plasmodium Liver Stage Infection Does Not Require Host De Novo Synthesized TAG and CE

Our lipidomic analyses revealed a significant enrichment in the neutral lipids TAG, CE, and DAG in *P. berghei*-infected cells at 25 hr after infection, although this was no longer the case at later time points (Figure 1B). Both TAG and CE are stored in organelles called lipid droplets (LDs) (Listenberger et al., 2003). During periods of increased lipogenesis, de-novo-synthesized or medium-derived fatty acids are channeled either into the glycerol-3-phosphate pathway to form DAG, which are then converted to TAG by DGAT1 or DGAT2 (Shi and Cheng 2009), or conjugated to free cholesterol by acyl-CoA: cholesterol acyltransferase (ACAT1/2) to form CE (Chang et al., 2001) (Figure S2). During periods of high-energy demand, fat stored in LDs is catabolized by neutral lipases to liberate free fatty acids (Figure S2). To assess the functional relevance of the observed changes, we first examined *P. berghei* infection in mice deficient in enzymes involved in CE and TAG synthesis. *P. berghei* load was similar in the livers of *ACAT1*$^{-/-}$ and *ACAT2*$^{-/-}$, when compared to littermate wild-type (WT) controls (Figure S2). Additionally, knockdown of *DGAT1* and *DGAT2* using siRNA in Huh7 cells did not influence the level of infection (Figure S2), in spite of a strong reduction in both TAG and CE in cells with reduced expression of DGAT2 (Figure S2). Finally, due to the decline in TAGs at 35 hr and 45 hr after infection, we also determined whether hydrolysis of TAGs in *P. berghei*-infected cells could provide building blocks for pathways active at later stages of liver stage infection. However, *P. berghei* liver infection was not affected in mice deficient in ATGL (Zimmermann et al., 2004) when compared to WT controls, in spite of the visible increase in LD size and a significant accumulation of TAG, as shown by oil red O staining and MS analysis, respectively (Figure S2). Taken together, these data suggest that *Plasmodium* liver stage infection is independent of host CE biosynthesis and TAG biosynthetic and lipolytic pathways.

Both Arms of Host Cell De Novo PC Synthesis Contribute to *Plasmodium* Liver Stage Infection Persistence

Since PC was highly enriched in infected cells (Figures 1B and S1), we next investigated whether this phospholipid could play a role during *Plasmodium* intrahepatic parasitism. The bulk of PC (as well as PE) is synthesized by the Kennedy pathway for which choline phosphate cytidyltransferase (PCYTα or CTα) is the rate-limiting enzyme (Kennedy and Weiss 1956) (Figure 2A). Strikingly, downregulation of host cell CTα using siRNA in Huh7 cells (Figure S3) greatly reduced *P. berghei* infection (Figure 2A). The parasite liver load 48 hr after intraveneous injection of *P. berghei* sporozoites was also significantly lower in CTα liver-specific deficient mice (CTα-LKO) (Jacobs et al., 2004), as compared to that of CTα-flox littermate mice (Figure 2B). We further characterized the effect of CTα depletion on infection by immunofluorescence microscopy analysis of thick liver sections. The number of *P. berghei* exo-erythrocytic forms (EEFs) was significantly reduced in CTα-LKO liver sections compared to CTα-flox controls (Figure 2C), with no differences in EEF

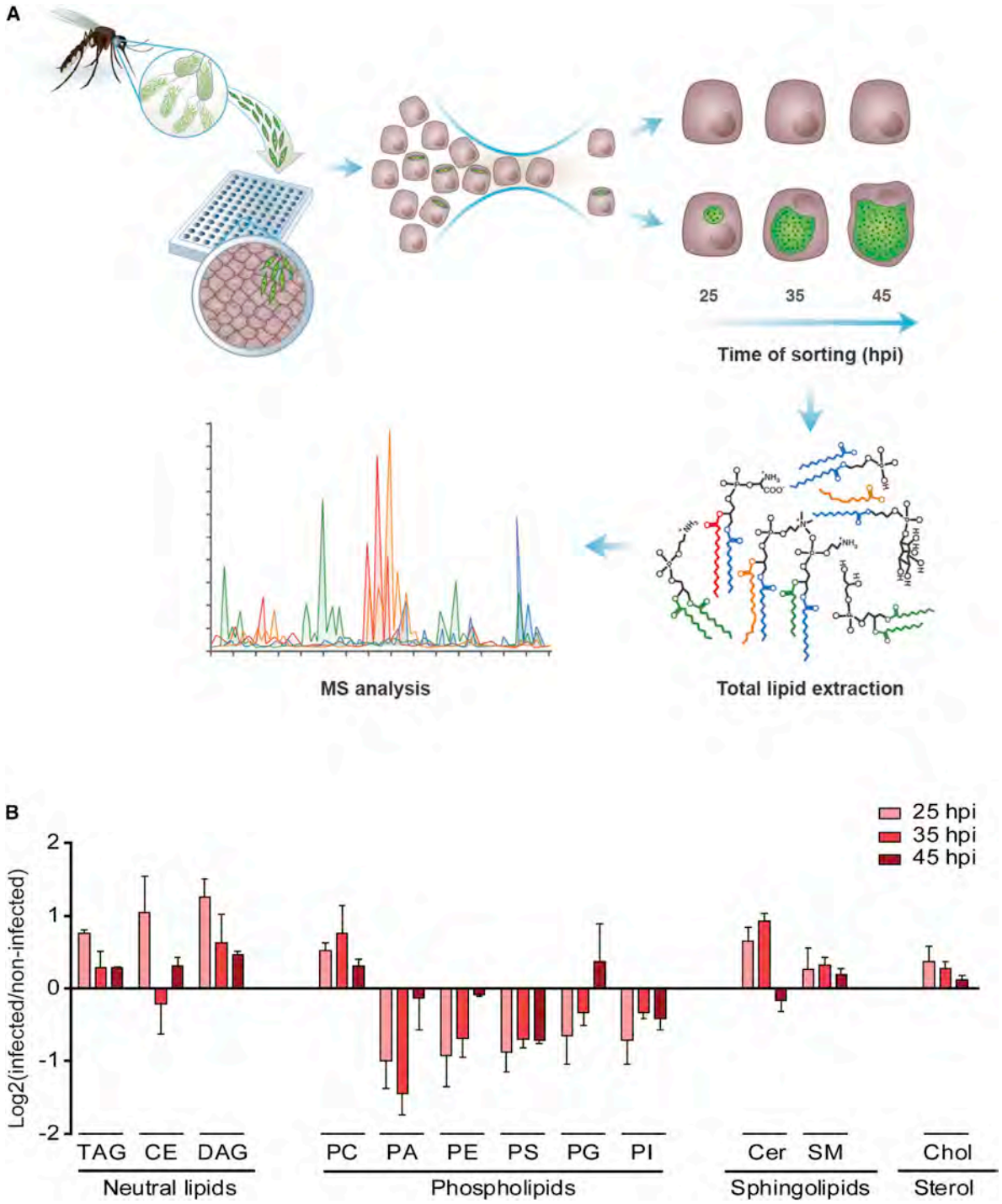

Figure 1. The Lipid Composition of *Plasmodium*-Infected Hepatoma Cells Is Altered during Infection

(A) Schematic representation of the approach for quantifying lipids in *P. berghei*-infected and noninfected cells: after FACS, cells were spiked with known concentrations of internal standards, and total cellular lipids were extracted and analyzed by shotgun ESI-MS.

(B) Relative abundance of major lipid classes in infected and noninfected cells at 25, 35, and 45 hr postinfection (hpi) are presented in $\log_2$ (infected/noninfected cells). Error bars represent SEM of each lipid from three to four biological replicates for each time point. Unpaired student t test was used to analyze statistical significance of differences in the abundance of each lipid in infected cells compared to noninfected cells at the same point: *$p < 0.05$

size (Figures 2D and 2E). Importantly, this effect on parasite numbers could not be ascribed to a defect in initial invasion of hepatocytes, as there was no difference in liver infection at 6 hpi between CTα-LKO and CTα-flox littermate mice (Figure 2F). The decrease in infection in CTα-LKO mice only became apparent at 24 hpi (Figure 2F).

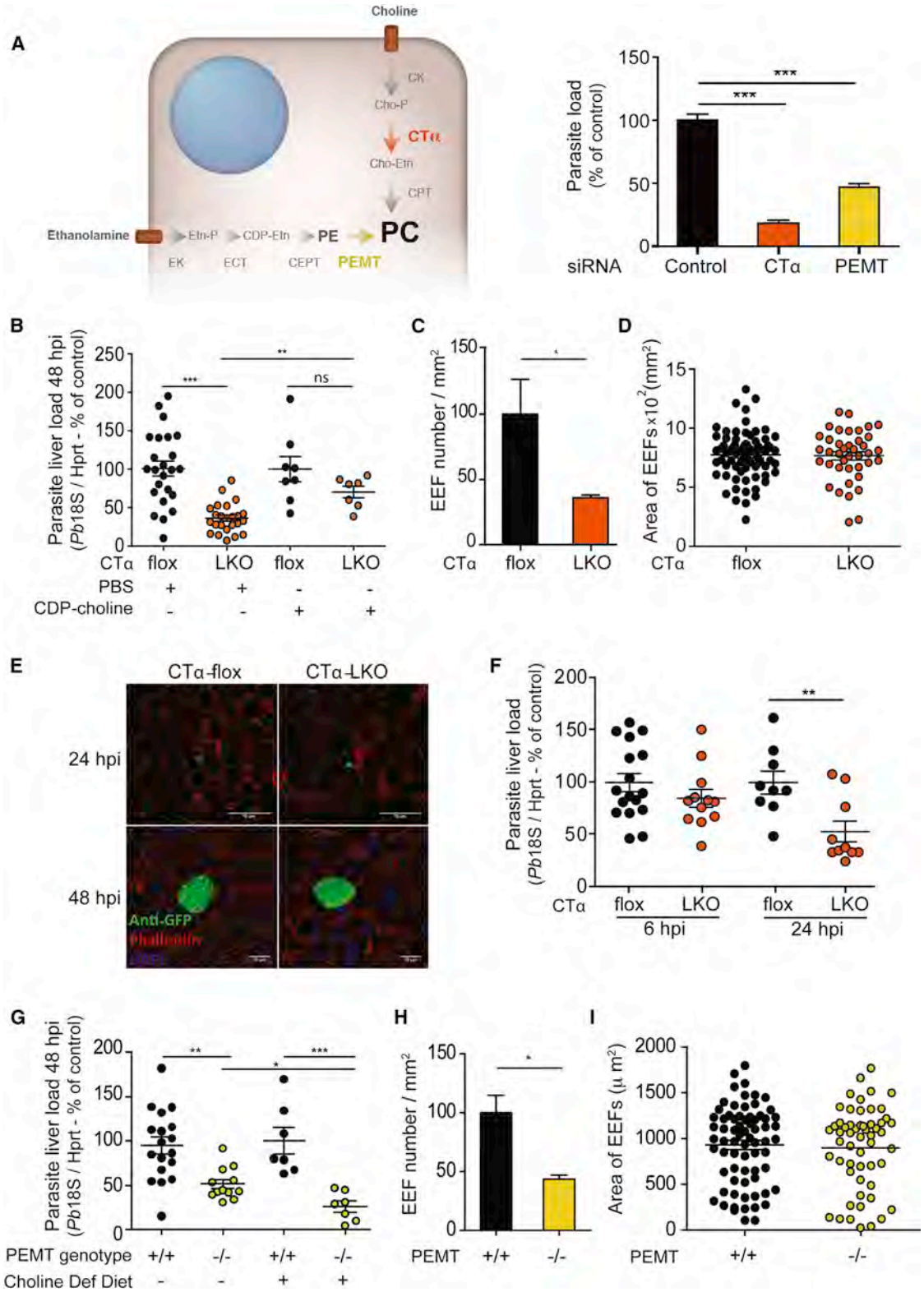

Figure 2. *P. berghei* Infection Is Significantly Impaired in CTα–Deficient Hepatocytes

(A) Huh7 cells were reverse transfected with control or siRNA specific to either CTα or PEMT, the two main enzymes involved in de novo host cell PC synthesis, and infected with luciferase-expressing *P. berghei* sporozoites. Parasite load (luminescence) was assessed after 48 hr and levels in CTα or PEMT knockdown cells were expressed as percentage of control siRNA-treated cells. Error bars represent SEM from three independent experiments. Mann Whitney test: ***p < 0.0001.

(legend continued on next page)

In addition to the Kennedy pathway, the sequential trimethylation of PE by phosphatidylethanolamine *N*-methyltransferase (PEMT), which is predominantly expressed in the liver, contributes about 20% of de novo PC synthesis (Ridgway and Vance 1987). Downmodulation of PEMT using siRNA in Huh7 cells (Figure S3) led to a decrease in *P. berghei* infection (Figure 2A). Similarly, the livers of mice deficient in PEMT ($PEMT^{-/-}$) showed a decreased parasite load compared to WT littermates, as measured by qRT-PCR of *P. berghei* 18S rRNA (Figure 2G). As before, this reduction in parasite load correlated with a significant decrease in *P. berghei* numbers in the livers of $PEMT^{-/-}$ mice (Figure 2H), without any effect on EEF size (Figure 2I). In an attempt to disrupt both routes of PC biosynthesis, we used $PEMT^{-/-}$ mice fed on a choline-deficient diet. While a choline-deficient diet alone (administered to $PEMT^{+/+}$ mice) did not affect infection, it had a significant impact on parasite liver load in $PEMT^{-/-}$ mice (Figure 2G). On the other hand, exogenous administration of CDP-choline to CTα-LKO mice (Niebergall et al., 2011) was sufficient to revert the impairment of *P. berghei* liver infection caused by depletion of CTα (Figure 2B). Altogether, and despite the ability of *Plasmodium* to synthesize PC from choline scavenged from the host cell (Déchamps et al., 2010), our data clearly show that de novo PC synthesis by the host cell is essential for *Plasmodium* hepatocyte infection.

Plasmodium Parasites Take Up Host PC during Intracellular Development

We next employed click chemistry detection to assess usage and distribution of PC in *Plasmodium* EEFs at different time points after infection (see Experimental Procedures; Figure S4). Prelabeled Huh7 cells (with propargylcholine, alkyne-tagged choline) infected with *P. berghei* sporozoites were analyzed by confocal microscopy. Choline-containing products were seen not only within the EEF (Figure S4) but also in the parasite plasma membrane (PPM) and PVM, as confirmed by colocalization with circumsporozoite (CS) (Figure S4) and UIS4 (upregulated in sporozoites), PPM, and PVM proteins, respectively. Intense staining of lipid-rich regions was observed at later time points (40–48 hr) after infection, and as the parasite underwent schizogony, each daughter nucleus was surrounded by choline-stained membranes (Figure S4).

While these observations show that the parasite uses choline or choline-containing products from the host cell, it is possible that the parasite might take up free choline (and not PC) previously hydrolyzed from choline-containing molecules. Indeed, propargylcholine is metabolized to PC, ether-lysophosphatidylcholine and lyso-phosphatidylcholine (lyso-PC) (Jao et al., 2009). Thus, we next used a nonhydrolyzable ether-lyso-PC to determine whether *Plasmodium* is capable of using host PC directly. The pattern of ether-lyso-PC distribution was similar to that of propargylcholine described above (Figure 3A). These results establish that the parasite takes up PC from the host cell throughout infection and without prior hydrolysis. Subcellular characterization of the lipid-rich domains within EEFs revealed that these structures likely correspond to parasite endoplasmic reticulum (ER) and not the apicoplast, as evidenced by the colocalization of ether-lyso-PC with the *P. berghei* ER-resident protein Bip (Figure 3B) but not with the apicoplast-resident protein ATG8 (Figure 3C). Additionally, ether-lyso-PC prelabeling of HepG2 cells, which support efficient merosome release upon PVM breakdown as it occurs in malaria infections in vivo, shows that host PC associates with PPM/PVM, intravacuolar membranous structures, and individual merozoites visualized by immune staining with anti-MSP1 antibodies (Figure S4). Click labeling on live detached merosomes also showed distinct propargylcholine staining of individual merozoites (Figure S4). Uptake of PC from the host cell into *P. berghei* EEFs was also observed in mouse primary hepatocytes (Figure S4). Similar results were obtained when an azido-tetramethylrhodamine was used in the click cyclo-addition reaction instead of azido-sulfo-bodipy, showing that the reporter fluorophore does not affect the pattern of PC distribution (Figure S4). Next, we assessed whether the use of PC from host cell also occurs during pre-erythrocytic development of the human pathogen *P. falciparum* in micropatterned human primary hepatocytes (March et al., 2013). Host-derived PC associated with *P. falciparum* EEFs as early as 1.5 days after infection, with a distinct perinuclear staining in all EEFs examined (Figure 3D).

Host Cell PC Contributes to PVM Integrity

We next sought to determine the mechanism by which host PC contributes to the establishment of parasite infection in

(B) CTα-floxed and CTα liver-specific knockout (LKO) mice were infected with 5×10^4 GFP-expressing *P. berghei* sporozoites, and the parasite load in the liver at 48 hr after infection was determined by qRT-PCR of *Pb*18S rRNA normalized to HPRT and expressed as percentage of controls. CTα-floxed n = 24, CTα liver-specific knockout (LKO) n = 24. Both CTα-floxed and CTα liver-specific knockout (LKO) mice were injected with CDP-choline (1mg/Kg mouse) intraperitoneally daily for 7 days prior to infection and daily after infection (CTα-floxed n = 8, LKO n = 7). Controls included mice that were injected with PBS (vehicle) intraperitoneally at the same times of CDP-choline administration. Mice were sacrificed at 48 hr after infection, and liver load was quantified as above. Error bars represent SEM. Mann Whitney test: $^{**}p < 0.001$ and $^{***}p < 0.0001$.

(C and D) Quantification of liver burden (number of EEFs per area of liver) and EEF size, respectively, at 48 hr after infection by fluorescence microscopy.

(E) Representative confocal images of EEFs in CTα-floxed versus CTα-LKO liver sections at 24 and 48 hpi. Parasites were stained with an anti-GFP antibody (green), F-actin was labeled with phalloidin 555 (red), and DNA was labelled with DAPI (blue). Scale bar, 10 μm.

(F) Parasite load in the livers of CTα-floxed versus CTα-LKO mice at 6 (n = 17 and n = 12, respectively) and 24 hr (n = 9, n = 10 respectively) after infection with 5×10^4 GFP-expressing *P. berghei* sporozoites, as measured by qRT-PCR of 18S rRNA normalized to HPRT and expressed as a percentage of controls. Mann Whitney test: $^{**}p < 0.001$, ns = not significant

(G) PEMT WT ($PEMT^{+/+}$) and PEMT-deficient mice ($PEMT^{-/-}$) on placebo (n = 18, n = 12 respectively) or choline-deficient diets (n = 7, n = 7 respectively) were infected with 5×10^4 GFP-expressing *P. berghei* sporozoites and parasite liver load quantified at 48 hr after infection by RT-PCR of 18S rRNA normalized to HPRT and expressed as percentage of WT in each condition. Error bars represent SEM. Mann Whitney test: $^{**}p < 0.001$ and $^{***}p < 0.0001$.

(H and I) Quantification of parasite burden and the area of EEFs in liver sections from $PEMT^{+/+}$ and $PEMT^{-/-}$ mice on placebo diet after immunostaining with anti-GFP antibodies and confocal imaging.

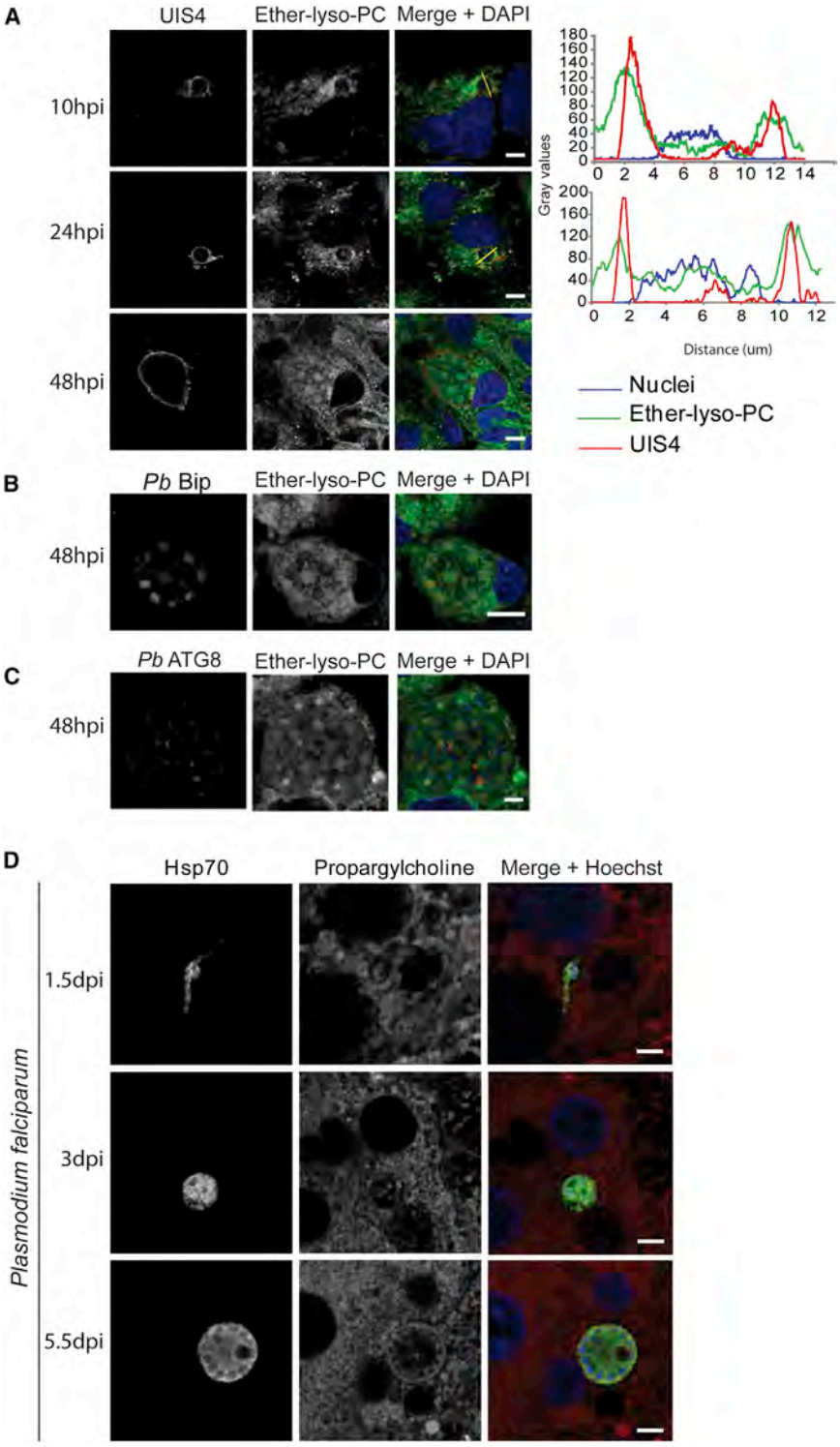

Figure 3. Ether-lyso PC/Choline-Containing Lipids from the Host Associate with *Plasmodium* Membranous Structures throughout Liver Stage Infection

(A–C) Huh7 hepatoma cells were prelabeled with ether-lyso-PC; infected with RFP-expressing *P. berghei* ANKA sporozoites; and fixed at 10, 24, and 48 hr after infection. The cells were immunostained with anti-UIS4 (red) (A), anti-*Pb*Bip (red) (B), anti-*Pb*ATG8 (C), and DAPI. Click labeling was performed with azido-bodipy (green) (see Figure S4A), and confocal images were acquired. Plot profiles of UIS4 (red), ether-lyso-PC (green), and DAPI (blue) intensity (gray values) distributions across EEFs are shown at 10 and 24 hpi.

(D) Primary human hepatocytes were prelabeled with propargylcholine; infected with *P. falciparum* sporozoites; and fixed at 1.5, 3, and 5.5 days postinfection (dpi). Parasites were immunostained with anti-*Pf*Hsp70 (green), and Click reaction was performed with Alexa-Fluor 594 conjugated azide (red). Confocal images were acquired with a laser scanning microscope. Scale bar, 10 μm.

hepatocytes. Several studies using distinct knockout parasites lines that exhibit defects in PVM formation and remodeling show a decrease in the number of parasites able to complete liver stage development (Aly et al., 2008; Ishino et al., 2005; Labaied et al., 2007; Mueller et al., 2005a, 2005b, Silvie et al., 2008; van Dijk et al., 2005; van Schaijk et al., 2008). Additionally, we have recently shown that treatment of liver stage parasites with a class of drugs called torins impairs trafficking of *Plasmodium* PVM-resident proteins resulting in elimination of those parasites (Hanson et al., 2013). Given our observations that host PC localizes to the PVM throughout infection and that parasite numbers decrease sharply when the PC-biosynthetic activity of the host cell is compromised, we hypothesized that reduction of PC at the PVM might impair the insertion and/or maintenance of *Plasmodium* PVM-resident proteins, leading to parasite elimination. Indeed, it is well established that the PC/PE ratio in membranes affects the membrane protein content (Li et al., 2006). Thus, we next analyzed the expression of UIS4, a *Plasmodium* protein known to localize to the PVM and to be essential during liver stage (Mueller et al., 2005b), in primary hepatocytes deficient for CTα. The amount of UIS4 was significantly reduced in the PVM of CTα-deficient hepatocytes, when compared to WT hepatocytes (Figures 4A and 4B), in spite of similar transcriptional expression of the *uis4* gene (Figure 4C). Thus, our data suggest that the insertion of host PC into the PVM is critical for the parasite to maintain the protein composition of this essential membrane and avoid host cell intrinsic elimination mechanisms.

DISCUSSION

How *Plasmodium* parasites modulate the host cell environment during the liver stage, in order to survive long enough to generate

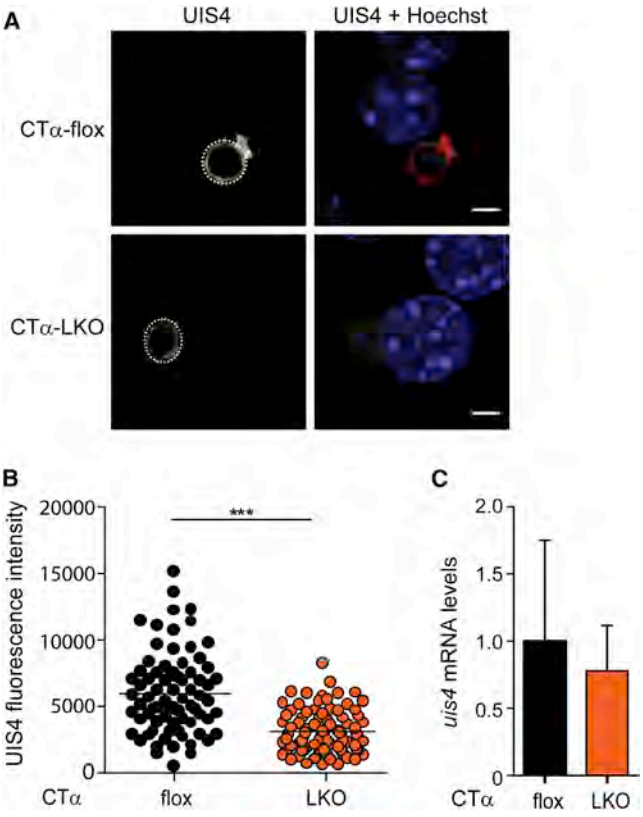

Figure 4. UIS4 Protein Levels Are Significantly Reduced in *Plasmodium* EEFs in Mouse Primary Hepatocytes with Impaired PC Biosynthesis

(A) Confocal images of *P. berghei* EEFs at 18 hpi in primary hepatocytes from CTα-flox and CTα-LKO mice; UIS4 (red) and nuclei (blue). Dotted circles around EEFs indicate the regions of interest for which UIS4 signal was measured ([B] below). Scale bar, 10 μm.

(B) UIS4 signal intensity on EEFs at 18 hpi in primary hepatocytes from CTα-flox and CTα-LKO mice. Mann Whitney test: ***$p < 0.0001$.

(C) Quantification of UIS4 transcriptional expression by qRT-PCR in the livers of CTα-flox and CTα-LKO mice infected with *P. berghei* parasites.

the large numbers of merozoites that are released into the blood, is still poorly understood. Inside each invaded hepatocyte, a single sporozoite generates thousands of new merozoites. This rapid proliferation rate implies that sufficient lipids are available to support both the enlargement of the PVM and membrane neogenesis for newly formed merozoites. We hypothesized that the inherent ability of hepatocytes to mobilize lipids may be critical during *Plasmodium* infection of the liver. Our quantitative determination of the lipid composition of *P. berghei*-infected hepatocytes at different time points after initial infection revealed that PC is the only phospholipid enriched in relative abundance in infected cells with a concomitant decline in the relative abundance of PE, PS, PA, and PI. In addition, confocal microscopy showed that *Plasmodium* parasites continuously accumulate host PC. Using target-specific siRNAs, in addition to CTα- and PEMT-deficient mice, we showed that the host de novo PC biosynthetic machinery is indispensable for *Plasmodium* intrahepatic infection, despite its ability to synthesize PC de novo (Déchamps et al., 2010).

Our data show that intracellular development of the parasite correlates with increased synthesis of the major structural phospholipid, PC, both through the Kennedy and the PEMT pathways, but PS decarboxylase activity does not seem to be required, as PE and PS levels declined at all time points examined. Considering that PC is the major structural phospholipid of eukaryotic membranes and that host PC is used by the parasite throughout infection, it was surprising that, despite a profound impairment in parasite survival, knockout of CTα did not affect parasite growth or merozoite formation. These observations suggest that compensatory PC biosynthetic pathways, such as the PEMT and Lands cycle (Lands 1958; Ridgway and Vance 1987), or other proteins either from the host or parasite side might be engaged during this process.

Also surprising is the fact that while the lipidomics data show a significant increase in lipids typically associated with LDs (namely TAG and CE), an organelle used by many pathogens as a source of structural lipids and energy (Chandak et al., 2010; Cocchiaro et al., 2008; Kumar et al., 2006; Miyanari et al., 2007), ablation of key enzymes involved in CE and TAG synthesis or lipolysis does not disturb any aspect of the infection. LD biogenesis represents a conserved cellular response to infection (Melo and Dvorak 2012) in macrophages but does not seem to play a direct role in *Plasmodium* infection of hepatocytes.

The exo-erythrocytic stage of *Plasmodium* infection occurs within host hepatocytes, a cell type with a phenomenal capacity to support lipid metabolism. Notably, lack of de novo synthesis of a single phospholipid, PC, in the host cell strongly affects parasite survival inside hepatocytes. We show that reduction of PC availability directly reflects on the protein composition of the PVM, as noted by a significant decrease on the levels of the PVM-resident protein UIS4, which implicates PC in PVM remodeling. Given that host PC was found to colocalize with the parasite ER, another plausible scenario is that PC depletion affects the trafficking of proteins to the parasite surface. We cannot exclude that other mechanisms might be in place to explain why host PC is so important for infection. Still, the PVM constitutes the critical interface between the parasite and a potentially hostile host cell environment, and the presence of *Plasmodium* proteins on the PVM was shown to be indispensable for the parasite to avoid elimination by the host cell (Hanson et al., 2013), providing a likely explanation as to why host PC plays such a critical role in parasite survival.

EXPERIMENTAL PROCEDURES

Mice

C57BL6 mice were purchased from Jackson laboratory, and all experiments were performed in strict compliance to the guidelines of our institution's animal ethics committee and the Federation of European Laboratory Animal Science Associations (FELASA).

Cells

HepG2, Huh7 cells, and primary hepatocytes were cultured in supplemented Dulbecco's modified Eagle's medium (DMEM), RPMI 1640, and William's medium, respectively, as described in Liehl et al. (2014), and maintained in a 5% CO_2 humidified incubator at 37°C.

Parasites and Infections

GFP-, RFP-, or luciferase-expressing *P. berghei* sporozoites were dissected from salivary glands of infected female *Anopheles stephensi* mosquitoes into

DMEM medium prior to be added to cells or injected into mice for in vitro and in vivo infections. Infection in vitro was assessed as previously described using a multiplate reader (Infinite M200 from Tecan, Switzerland) or a BD LSR Fortessa cytometer (Franke-Fayard et al., 2004; Ploemen et al., 2009; Prudêncio et al., 2008).

Total Lipid Extraction and Quantitative Mass Spectrometry Analysis of Infected and Noninfected Cells

Noninfected and GFP-expressing *P. berghei*-infected cells were gated on the basis of their different fluorescence intensity as previously established (Albuquerque et al., 2009; Prudêncio et al., 2008). Cells were collected by FACS sorting, and total cellular lipid was extracted from sorted cells as previously described (Sampaio et al., 2011).

siRNA

Human Huh7 hepatoma cells were reverse transfected with 30 nM of target-specific or control siRNA sequences (Table S2) according to the manufacturer's instructions (Ambion, Life technologies). The efficiency of knockdown was assessed by quantitative RT-PCR (Table S3).

Imaging PC in *P. berghei*-Infected Hepatocytes

Host cells seeded on glass coverslips were metabolically prelabeled with 500 μM propargylcholine or 20 μM of a nonhydrolyzable PC, ether-lyso-PC (Kuerschner et al., 2012), for 8–12 hr. Cells were then infected with RFP-expressing *P. berghei* ANKA sporozoites, as previously described. After fixation, click cyclo-addition reaction with Sulfo-Azido-Bodipy was carried out as described elsewhere (Gaebler et al., 2013; Jao et al., 2009).

Statistical Analysis

Statistical analyses were performed using GraphPad Prism 5 software. Student t test was used for significance of differences observed for. * $p < 0.05$, ** $p < 0.01$, and *** $p < 0.0001$.

SUPPLEMENTAL INFORMATION

Supplemental Information includes four figures, three tables, and Supplemental Experimental Procedures and can be found with this article online at http://dx.doi.org/10.1016/j.chom.2014.11.006.

ACKNOWLEDGMENTS

We would like to thank Dennis Vance (Alberta University, Canada) for generously providing the CTα- and PEMT-deficient mice, Robert Farese for providing ACAT1- and ACAT2-deficient mice (University of California, USA), Rudolf Zechner (University of Graz, Austria) for providing ATGL-deficient mice, Volker Heussler (University of Bern, Switzerland) for providing *Pb*ATG8 antibodies, and Ana Parreira for producing the *P. berghei*-infected *Anopheles* mosquitoes. This work was supported by the European Research Council under the EUs Seventh Framework Programme ERC *grant agreement* n° 311502 (to MMM) and Fundação para a Ciência e Tecnologia (FCT; grants EXCL/IMI-MIC/0056/2012 and PTDC/IMI-MIC/1568/2012). M.A.I. was sponsored by FP7—Marie Curie Actions Initial Training Networks—"Interventions strategies against malaria" InterMal Training fellowship PITN-GA-2008-215281. F.F. was funded by Chica and Heinz Schaller Foundation EVIMalaR. G.C. was the recipient of a Marie Curie (PIEF-GA-2009-235864) and FCT (SFRH/BPD/74151/2010) fellowships. E.R. was the recipient of EMBO (ALTF 949-2008) and FCT (SFRH/BPD/68709/2010) fellowships. V.L. was sponsored by EMBO (ALTF 357-2009) and FCT (BPD-81953-2011).

Received: June 12, 2014
Revised: September 29, 2014
Accepted: November 4, 2014
Published: December 10, 2014

REFERENCES

Albuquerque, S.S., Carret, C., Grosso, A.R., Tarun, A.S., Peng, X., Kappe, S.H., Prudêncio, M., and Mota, M.M. (2009). Host cell transcriptional profiling during malaria liver stage infection reveals a coordinated and sequential set of biological events. BMC Genomics *10*, 270.

Allary, M., Lu, J.Z., Zhu, L., and Prigge, S.T. (2007). Scavenging of the cofactor lipoate is essential for the survival of the malaria parasite Plasmodium falciparum. Mol. Microbiol. *63*, 1331–1344.

Aly, A.S., Mikolajczak, S.A., Rivera, H.S., Camargo, N., Jacobs-Lorena, V., Labaied, M., Coppens, I., and Kappe, S.H. (2008). Targeted deletion of SAP1 abolishes the expression of infectivity factors necessary for successful malaria parasite liver infection. Mol. Microbiol. *69*, 152–163.

Bohdanowicz, M., and Grinstein, S. (2013). Role of phospholipids in endocytosis, phagocytosis, and macropinocytosis. Physiol. Rev. *93*, 69–106.

Chandak, P.G., Radovic, B., Aflaki, E., Kolb, D., Buchebner, M., Fröhlich, E., Magnes, C., Sinner, F., Haemmerle, G., Zechner, R., et al. (2010). Efficient phagocytosis requires triacylglycerol hydrolysis by adipose triglyceride lipase. J. Biol. Chem. *285*, 20192–20201.

Chang, T.Y., Chang, C.C., Lin, S., Yu, C., Li, B.L., and Miyazaki, A. (2001). Roles of acyl-coenzyme A:cholesterol acyltransferase-1 and -2. Curr. Opin. Lipidol. *12*, 289–296.

Cocchiaro, J.L., Kumar, Y., Fischer, E.R., Hackstadt, T., and Valdivia, R.H. (2008). Cytoplasmic lipid droplets are translocated into the lumen of the Chlamydia trachomatis parasitophorous vacuole. Proc. Natl. Acad. Sci. USA *105*, 9379–9384.

Déchamps, S., Shastri, S., Wengelnik, K., and Vial, H.J. (2010). Glycerophospholipid acquisition in Plasmodium - a puzzling assembly of biosynthetic pathways. Int. J. Parasitol. *40*, 1347–1365.

Deschermeier, C., Hecht, L.S., Bach, F., Rützel, K., Stanway, R.R., Nagel, A., Seeber, F., and Heussler, V.T. (2012). Mitochondrial lipoic acid scavenging is essential for Plasmodium berghei liver stage development. Cell. Microbiol. *14*, 416–430.

Franke-Fayard, B., Trueman, H., Ramesar, J., Mendoza, J., van der Keur, M., van der Linden, R., Sinden, R.E., Waters, A.P., and Janse, C.J. (2004). A Plasmodium berghei reference line that constitutively expresses GFP at a high level throughout the complete life cycle. Mol. Biochem. Parasitol. *137*, 23–33.

Gaebler, A., Milan, R., Straub, L., Hoelper, D., Kuerschner, L., and Thiele, C. (2013). Alkyne lipids as substrates for click chemistry-based in vitro enzymatic assays. J. Lipid Res. *54*, 2282–2290.

Hanson, K.K., Ressurreição, A.S., Buchholz, K., Prudêncio, M., Herman-Ornelas, J.D., Rebelo, M., Beatty, W.L., Wirth, D.F., Hänscheid, T., Moreira, R., et al. (2013). Torins are potent antimalarials that block replenishment of Plasmodium liver stage parasitophorous vacuole membrane proteins. Proc. Natl. Acad. Sci. USA *110*, E2838–E2847.

Ishino, T., Chinzei, Y., and Yuda, M. (2005). Two proteins with 6-cys motifs are required for malarial parasites to commit to infection of the hepatocyte. Mol. Microbiol. *58*, 1264–1275.

Jacobs, R.L., Devlin, C., Tabas, I., and Vance, D.E. (2004). Targeted deletion of hepatic CTP:phosphocholine cytidylyltransferase alpha in mice decreases plasma high density and very low density lipoproteins. J. Biol. Chem. *279*, 47402–47410.

Jao, C.Y., Roth, M., Welti, R., and Salic, A. (2009). Metabolic labeling and direct imaging of choline phospholipids in vivo. Proc. Natl. Acad. Sci. USA *106*, 15332–15337.

Kennedy, E.P., and Weiss, S.B. (1956). The function of cytidine coenzymes in the biosynthesis of phospholipides. J. Biol. Chem. *222*, 193–214.

Kuerschner, L., Richter, D., Hannibal-Bach, H.K., Gaebler, A., Shevchenko, A., Ejsing, C.S., and Thiele, C. (2012). Exogenous ether lipids predominantly target mitochondria. PLoS ONE *7*, e31342.

Kumar, Y., Cocchiaro, J., and Valdivia, R.H. (2006). The obligate intracellular pathogen Chlamydia trachomatis targets host lipid droplets. Curr. Biol. *16*, 1646–1651.

Labaied, M., Harupa, A., Dumpit, R.F., Coppens, I., Mikolajczak, S.A., and Kappe, S.H. (2007). Plasmodium yoelii sporozoites with simultaneous deletion of P52 and P36 are completely attenuated and confer sterile immunity against infection. Infect. Immun. *75*, 3758–3768.

Lands, W.E. (1958). Metabolism of glycerolipides; a comparison of lecithin and triglyceride synthesis. J. Biol. Chem. *231*, 883–888.

Li, Z., Agellon, L.B., Allen, T.M., Umeda, M., Jewell, L., Mason, A., and Vance, D.E. (2006). The ratio of phosphatidylcholine to phosphatidylethanolamine influences membrane integrity and steatohepatitis. Cell Metab. *3*, 321–331.

Liehl, P., Zuzarte-Luís, V., Chan, J., Zillinger, T., Baptista, F., Carapau, D., Konert, M., Hanson, K.K., Carret, C., Lassnig, C., et al. (2014). Host-cell sensors for Plasmodium activate innate immunity against liver-stage infection. Nat. Med. *20*, 47–53.

Lindner, S.E., Sartain, M.J., Hayes, K., Harupa, A., Moritz, R.L., Kappe, S.H., and Vaughan, A.M. (2014). Enzymes involved in plastid-targeted phosphatidic acid synthesis are essential for Plasmodium yoelii liver-stage development. Mol. Microbiol. *91*, 679–693.

Listenberger, L.L., Han, X., Lewis, S.E., Cases, S., Farese, R.V., Jr., Ory, D.S., and Schaffer, J.E. (2003). Triglyceride accumulation protects against fatty acid-induced lipotoxicity. Proc. Natl. Acad. Sci. USA *100*, 3077–3082.

March, S., Ng, S., Velmurugan, S., Galstian, A., Shan, J., Logan, D.J., Carpenter, A.E., Thomas, D., Sim, B.K., Mota, M.M., et al. (2013). A microscale human liver platform that supports the hepatic stages of Plasmodium falciparum and vivax. Cell Host Microbe *14*, 104–115.

Melo, R.C., and Dvorak, A.M. (2012). Lipid body-phagosome interaction in macrophages during infectious diseases: host defense or pathogen survival strategy? PLoS Pathog. *8*, e1002729.

Miyanari, Y., Atsuzawa, K., Usuda, N., Watashi, K., Hishiki, T., Zayas, M., Bartenschlager, R., Wakita, T., Hijikata, M., and Shimotohno, K. (2007). The lipid droplet is an important organelle for hepatitis C virus production. Nat. Cell Biol. *9*, 1089–1097.

Mueller, A.K., Labaied, M., Kappe, S.H., and Matuschewski, K. (2005a). Genetically modified Plasmodium parasites as a protective experimental malaria vaccine. Nature *433*, 164–167.

Mueller, A.K., Camargo, N., Kaiser, K., Andorfer, C., Frevert, U., Matuschewski, K., and Kappe, S.H. (2005b). Plasmodium liver stage developmental arrest by depletion of a protein at the parasite-host interface. Proc. Natl. Acad. Sci. USA *102*, 3022–3027.

Niebergall, L.J., Jacobs, R.L., Chaba, T., and Vance, D.E. (2011). Phosphatidylcholine protects against steatosis in mice but not non-alcoholic steatohepatitis. Biochim. Biophys. Acta *1811*, 1177–1185.

Pei, Y., Tarun, A.S., Vaughan, A.M., Herman, R.W., Soliman, J.M., Erickson-Wayman, A., and Kappe, S.H. (2010). Plasmodium pyruvate dehydrogenase activity is only essential for the parasite's progression from liver infection to blood infection. Mol. Microbiol. *75*, 957–971.

Ploemen, I.H., Prudêncio, M., Douradinha, B.G., Ramesar, J., Fonager, J., van Gemert, G.J., Luty, A.J., Hermsen, C.C., Sauerwein, R.W., Baptista, F.G., et al. (2009). Visualisation and quantitative analysis of the rodent malaria liver stage by real time imaging. PLoS ONE *4*, e7881.

Prudêncio, M., Rodriguez, A., and Mota, M.M. (2006). The silent path to thousands of merozoites: the Plasmodium liver stage. Nat. Rev. Microbiol. *4*, 849–856.

Prudêncio, M., Rodrigues, C.D., Ataíde, R., and Mota, M.M. (2008). Dissecting in vitro host cell infection by Plasmodium sporozoites using flow cytometry. Cell. Microbiol. *10*, 218–224.

Ralph, S.A., van Dooren, G.G., Waller, R.F., Crawford, M.J., Fraunholz, M.J., Foth, B.J., Tonkin, C.J., Roos, D.S., and McFadden, G.I. (2004). Tropical infectious diseases: metabolic maps and functions of the Plasmodium falciparum apicoplast. Nat. Rev. Microbiol. *2*, 203–216.

Ridgway, N.D., and Vance, D.E. (1987). Purification of phosphatidylethanolamine N-methyltransferase from rat liver. J. Biol. Chem. *262*, 17231–17239.

Rodrigues, C.D., Hannus, M., Prudêncio, M., Martin, C., Gonçalves, L.A., Portugal, S., Epiphanio, S., Akinc, A., Hadwiger, P., Jahn-Hofmann, K., et al. (2008). Host scavenger receptor SR-BI plays a dual role in the establishment of malaria parasite liver infection. Cell Host Microbe *4*, 271–282.

Sampaio, J.L., Gerl, M.J., Klose, C., Ejsing, C.S., Beug, H., Simons, K., and Shevchenko, A. (2011). Membrane lipidome of an epithelial cell line. Proc. Natl. Acad. Sci. USA *108*, 1903–1907.

Shi, Y., and Cheng, D. (2009). Beyond triglyceride synthesis: the dynamic functional roles of MGAT and DGAT enzymes in energy metabolism. Am. J. Physiol. Endocrinol. Metab. *297*, E10–E18.

Silvie, O., Goetz, K., and Matuschewski, K. (2008). A sporozoite asparagine-rich protein controls initiation of Plasmodium liver stage development. PLoS Pathog. *4*, e1000086.

Tarun, A.S., Peng, X., Dumpit, R.F., Ogata, Y., Silva-Rivera, H., Camargo, N., Daly, T.M., Bergman, L.W., and Kappe, S.H. (2008). A combined transcriptome and proteome survey of malaria parasite liver stages. Proc. Natl. Acad. Sci. USA *105*, 305–310.

van Dijk, M.R., Douradinha, B., Franke-Fayard, B., Heussler, V., van Dooren, M.W., van Schaijk, B., van Gemert, G.J., Sauerwein, R.W., Mota, M.M., Waters, A.P., and Janse, C.J. (2005). Genetically attenuated, P36p-deficient malarial sporozoites induce protective immunity and apoptosis of infected liver cells. Proc. Natl. Acad. Sci. USA *102*, 12194–12199.

van Meer, G., and Sprong, H. (2004). Membrane lipids and vesicular traffic. Curr. Opin. Cell Biol. *16*, 373–378.

van Meer, G., Voelker, D.R., and Feigenson, G.W. (2008). Membrane lipids: where they are and how they behave. Nat. Rev. Mol. Cell Biol. *9*, 112–124.

van Schaijk, B.C., Janse, C.J., van Gemert, G.J., van Dijk, M.R., Gego, A., Franetich, J.F., van de Vegte-Bolmer, M., Yalaoui, S., Silvie, O., Hoffman, S.L., et al. (2008). Gene disruption of Plasmodium falciparum p52 results in attenuation of malaria liver stage development in cultured primary human hepatocytes. PLoS ONE *3*, e3549.

Vaughan, A.M., O'Neill, M.T., Tarun, A.S., Camargo, N., Phuong, T.M., Aly, A.S., Cowman, A.F., and Kappe, S.H. (2009). Type II fatty acid synthesis is essential only for malaria parasite late liver stage development. Cell. Microbiol. *11*, 506–520.

Yalaoui, S., Huby, T., Franetich, J.F., Gego, A., Rametti, A., Moreau, M., Collet, X., Siau, A., van Gemert, G.J., Sauerwein, R.W., et al. (2008). Scavenger receptor BI boosts hepatocyte permissiveness to Plasmodium infection. Cell Host Microbe *4*, 283–292.

Yu, M., Kumar, T.R., Nkrumah, L.J., Coppi, A., Retzlaff, S., Li, C.D., Kelly, B.J., Moura, P.A., Lakshmanan, V., Freundlich, J.S., et al. (2008). The fatty acid biosynthesis enzyme FabI plays a key role in the development of liver-stage malarial parasites. Cell Host Microbe *4*, 567–578.

Zimmermann, R., Strauss, J.G., Haemmerle, G., Schoiswohl, G., Birner-Gruenberger, R., Riederer, M., Lass, A., Neuberger, G., Eisenhaber, F., Hermetter, A., and Zechner, R. (2004). Fat mobilization in adipose tissue is promoted by adipose triglyceride lipase. Science *306*, 1383–1386.

Cell Host & Microbe, Volume *16*

Supplemental Information

Host Cell Phosphatidylcholine Is a Key Mediator of Malaria Parasite Survival during Liver Stage Infection

Maurice A. Itoe, Júlio L. Sampaio, Ghislain G. Cabal, Eliana Real, Vanessa Zuzarte-Luis, Sandra March, Sangeeta N. Bhatia, Friedrich Frischknecht, Christoph Thiele, Andrej Shevchenko, and Maria M. Mota

SUPPLEMENTAL EXPERIMENTAL PROCEDURES

Chemicals

RPMI 1640, DMEM, PBS pH 7.4, Tryspin, OptiMEM, and Lipofectamine RNAiMAX were purchased from Gibco Invitrogen. siRNAs were purchased from Ambion. All other chemicals, except specified were obtained from Sigma or Invitrogen

Animals

C57BL6 mice were purchased from Jackson laboratory and housed in a 12 hour night-light cycle. All transgenic mice were bred and housed in the same conditions. All animal experiments were performed in strict compliance to the guidelines of our institution´s animal ethics committee and the Federation of European Laboratory Animal Science Associations (FELASA).

Culturing of hepatoma cells, Huh7 and HepG2, and primary hepatocytes

HepG2 and Huh7 cells were cultured, respectively, in supplemented Dulbecco´s modified Eagle´s medium (DMEM) and RPMI 1640 medium. Primary hepatocytes were cultured in supplemented William´s medium E as described in (Liehl et al. 2014). All cells were maintained in a 5% CO_2 humidified incubator at 37°C.

Infection of hepatoma and mouse primary hepatocytes

GFP-, RFP-, or luciferase-expressing transgenic *P. berghei* sporozoites were dissected from salivary glands of infected female *Anopheles stephensi* mosquitoes into DMEM medium. Depending on the experimental design, 10000-50000 GFP-, RFP-, luciferase-expressing *P. berghei* sporozoites were re-suspended in an appropriate volume of culture medium supplemented with 0,02% Fungizone and added to cultured hepatoma or mouse primary hepatocytes in either 96- or 24-well plates. The plates were centrifuged at 3000 rpm for 5 minutes and further incubated at 37°C for 2, 24, and 48 hpi. For microscopy, cells were seeded on glass cover-slips in 24-well plates and infected with sporozoites as above.

Luminescence and Fluorescence activated cell-sorting (FACS) analyses of *P. berghei* infection

Upon infection of hepatoma cells or primary hepatocytes with luciferase-expressing or GFP-expressing transgenic *P. berghei* sporozoites, infection was assessed as previously described in (Franke-Fayard et al. 2004, Ploemen et al. 2009, Prudencio et al. 2008) using a multiplate reader (Infinite M200 from Tecan, Switzerland) and a BD LSR Fortessa cytometer, respectively.

Immunofluorescence detection of *P. berghei* in Huh7, HepG2, and mouse primary hepatocytes

For intracellular localization of *P. berghei* parasites in Huh7 and HepG2 cells or primary hepatocytes, cells were rinsed briefly with 1 x PBS and fixed immediately with 3.7% Para-Formladehyde (PFA) for 20 minutes at room temperature. The cells were washed three times for 5 minutes and then incubated in 0,1M glycine for 10 minutes. Cellular membranes were permeabilized with a 0.1% saponin solution for 20 minutes at room temperature. This was followed by three washes with PBS and further incubation in blocking solution, 1-2% Bovine serum albumin (BSA) with 0.05 % saponin for 1-2 hours at room temperature. Parasites were stained with a parasite specific anti-Hsp70 (2E6) antibody at a 1:300 dilution for 1 hour at room temperature and the cells were washed three times with blocking solution, followed by further incubation in a 1:400 dilution of an anti-mouse Alexa-Fluor 488 or Alexa-Fluor 594 secondary antibody. Further three washes were carried out with blocking solution in the presence of a 1:1000 dilution of 4´, 6-diamidino-2-phenylindole (DAPI) for nuclei staining. Cover slips were mounted on microscope slides with Fluoromount (SouthernBiotech) and confocal images were acquired using a Zeiss LSM 510 META confocal microscope with the following parameters: excitation with 405nm, Band Pass (BP): 420nm-480nm, excitation with 488nm, BP: 505nm-530nm, excitation with 594nm: Long Pass (LP): 615nm. Images were processed with Image J software.

Lipid droplet staining by Oil Red O

Alongside immuno-fluorescence detection of EEFs, lipid droplets were stained with either Oil Red O (Sigma Aldrich). Briefly, immuno-labelled cells were incubated with 0.2% Oil Red O in 60% isopropanol for 15-30 minutes at room temperature.

RNA extraction and quantification

RNA was extracted from cultured cells using either High Pure RNA Isolation kit (Roche) or Trizol Reagent (Invitrogen) according to the manufacturers´ instruction. The amount of RNA in a sample was assessed with a NanoDrop® ND-1000 Spectrophotometer machine.

cDNA synthesis and quantitative RT-PCR

cDNA was synthesized from 1µg of RNA using the Roche cDNA synthesis kit according to the manufacturer´s instructions. The cDNA was synthesized as follows: 25°C for 10 minutes, 55°C for 30 minutes, and 85°C for 5 minutes. Quantitative real time reverse transcription polymerase chain reaction (qRT-PCR) was performed in a 7500 Fast Applied Bioscience (AB) machine using SBGR kit as follows: 50°C for 2 minutes, 95°C for 10 minutes, 40 cycles at 95°C for 15 seconds and 60°C for 1 minute, melting stage was done at 95◦C for 15 seconds, 60◦C for 1 minute, and 95°C for 30 seconds. Mouse or human HPRT primers were used for normalisation as a house keeping gene in all experiments. The primers used in the study are provided in supplementary Table S2. For quantitative RT-PCR, the delta-delta CT relative quantification method was used.

***In vivo P. berghei* sporozoites infection and quantification of parasite liver load by qRT-PCR and microscopy**

For mouse liver parasite load quantification, wild type C57BL6/J, PEMT knockout, CTα-flox, CTα-liver-specific knockout mice were injected i.v. with 5x 10^4 GFP-expressing *P. berghei* sporozoites and livers were collected either at 6, 24, or 48-50hpi. For the CTα-flox and CTα-liver-specific knockout mice rescue experiment, mice were administered PBS only or CDP-choline (in 160µL of PBS, 1mg/Kg of mouse)(Sigma-Aldrich) by intra-peritoneal injection daily for a week

and during liver infection (Niebergall et al. 2011). Total RNA was extracted from livers and parasite 18sRNA was quantified by RT-PCR using primers specific to *P. berghei* 18sRNA. Mouse HPRT expression was used for normalisation. For microscopy, 50µm liver sections were incubated in permeabilization/blocking solution; 2% BSA, 0,3% Triton-X-100, in PBS, at room temperature for 1 h. The slices were further incubated in anti-GFP for 2 h, rinsed thoroughly and mounted on microscope slides using Fluoromount (SouthernBiotech). Confocal images were acquired with a Zeiss LSM 510 META confocal microscope and analysed with Image J software.

FACS-Sorting of *P. berghei*-infected and non-infected cells for lipid mass spectrometry analysis

Pre-seeded Huh7 cells in 12- or 24-well plates were infected, respectively, with $5x10^4$ or $10x10^4$ GFP-expressing *P.berghei* sporozoites as described above. At 25, 35, and 45 hours after infection, the cells were trypsinized for 5 minutes at 37°C, re-suspended in an appropriate volume of 10% FBS supplemented PBS and centrifuged at 1200 rpm for 5 minutes. The pellets were further re-suspended in an appropriate volume of 2% FBS-supplemented PBS. Non-infected and GFP-expressing transgenic *P. berghei*-infected cells were gated on the basis of their different fluorescence intensity as previously established (Albuquerque et al. 2009, Prudencio et al. 2008). Cells were collected sequentially; starting with about $2x10^4$-$3x10^4$ non-infected cells and followed by collection of the entire infected population present in the sample. Immediately after FACS-sorting, the cells were washed once by centrifugation with 150 mM ammonium bicarbonate solution. The resultant pellet was snap-frozen in liquid nitrogen and stored at -80°C until the samples were analysed.

siRNA

Human Huh7 hepatoma cells were reverse-transfected with 30nM of target specific or control siRNA sequences according to the manufacturer´s instructions (Ambion, Life technologies). The sequences used are provided in supplementary Table S3. After 24 h of transfection, the efficiency of knockdown was assessed by quantitative RT-PCR.

Metabolic labelling and imaging of propargylcholine and phospholipids (phosphatidylcholine) in *P. berghei*-infected hepatocytes

Hepatoma or primary hepatocytes seeded on glass coverslips were metabolically pre-labelled with 500μM propargylcholine or 20μM of a non-hydrolyzable phosphatidylcholine, ether-lyso-phosphatidylcholine (Kuerschner et al. 2012), for 8-12 hours. The cells were rinsed thoroughly three times in fresh culture medium, chased for 1 hour in complete medium and then infected with RFP expressing-expressing *P. berghei* ANKA sporozoites as previously described. At different time points after infection, cells were fixed with 3.7% PFA for 20 minutes at room temperature, followed by three successive 10 minute washes with PBS. Parasite plasma membrane resident proteins; CSP or MSP1 were labelled with mouse anti-CSP or anti-MSP1 primary antibodies for 1 h, washed thoroughly with blocking solution, and then incubated in anti-mouse Alexa-Fluor 488 or 594 secondary antibodies. Click cyclo-addition reaction with Sulfo-Azido-Bodipy was carried out as described elsewhere (Gaebler et al. 2013, Jao et al. 2009). The cells were washed thoroughly with PBS and nuclei were stained with DAPI. The cover slips were mounted on microscope slides with Fluoromount (SouthernBiotech) and confocal images were acquired using a Zeiss LSM 510 META confocal microscope using a 63X Oil objective.

Total lipid extraction and quantitative mass spectrometry analysis

Total cellular lipid was extracted from sorted cells as previously described (Sampaio et al. 2011). Briefly, the sample was dissolved in 200 μL of 150 mM of ammonium bicarbonate. Samples were spiked with 10 μL of internal standard lipid mixture. 10 μL of an internal lipid standard mixture provide a total spike of 20 pmol DAG 17:0–17:0, 20 pmol phosphatidic acid (PA) 17:0–17:0, 50 pmol PE 17:0–17:0, 10 pmol phosphatidylglycerol (PG) 17:0–17:0, 40 pmol phosphatidylserine (PS) 17:0–17:0, 40 pmol phosphatidylcholine (PC) 18:3–18:3, 50 pmol phosphatidylinositol (PI) 17:0–17:0, 20 pmol ceramide (Cer) 18:1;2/17:0;0, 40 pmol SM 18:1;2/17:0, 20 pmol galactosylceramide (GalCer) 18:1;2/12:0, 20 pmol lactosylceramide (LacCer) 18:1;2/12:0, 10 pmol Triacylglyceride (TAG) 12:0/12:0/12:0, 90 pmol Cholesterol-ester (CE) 17:0, 50 pmol Cholesterol-d7 (Chol). 265 μL of methanol were added to the mixture and

shaken for 10 minutes for homogenization. 730 µL of chloroform were added to the mixture and shaken for 1 h. The lower organic phase was collected and evaporated in a speedvac. Lipid extracts were dissolved in 100 µL of chloroform-methanol [1:2 (vol/vol)] and subjected to quantitative lipid analysis an LTQ-Orbitrap instrument (Thermo Fisher Scientific). Samples were infused with a TriVersa NanoMate robotic nanoflow ion source (Advion Biosciences, Inc.). DAG, PA, PS, PE, PI, and PG species were quantified by negative ion mode Fourier transform (FT) MS analysis on an LTQ-Orbitrap instrument multiple; PC, SM, ceramide, hexosylceramide, dihexosylceramide species were quantified by positive ion mode FT MS analysis on an LTQ-Orbitrap instrument as described elsewhere (Sampaio et al. 2011). Cholesterol was determined as described elsewhere (Liebisch et al. 2006).

Statistical analysis

Statistical analysis were performed using GraphPad Prism 5 software. Student t-test was used for significance of differences observed for. * $p < 0.05$, ** $p < 0.01$ and *** $p < 0.0001$.

REFERENCES

1. Albuquerque SS, Carret C, Grosso AR, Tarun AS, Peng X, Kappe SH, Prudencio M, Mota MM. 2009. Host cell transcriptional profiling during malaria liver stage infection reveals a coordinated and sequential set of biological events. BMC Genomics 10: 270.
2. Franke-Fayard B, Trueman H, Ramesar J, Mendoza J, van der Keur M, van der Linden R, Sinden RE, Waters AP, Janse CJ. 2004. A Plasmodium berghei reference line that constitutively expresses GFP at a high level throughout the complete life cycle. Mol Biochem Parasitol 137: 23-33.
3. Gaebler A, Milan R, Straub L, Hoelper D, Kuerschner L, Thiele C. 2013. Alkyne lipids as substrates for click chemistry-based in vitro enzymatic assays. J Lipid Res 54: 2282-2290.
4. Jao CY, Roth M, Welti R, Salic A. 2009. Metabolic labeling and direct imaging of choline phospholipids in vivo. Proc Natl Acad Sci U S A 106: 15332-15337.
5. Kuerschner L, Richter D, Hannibal-Bach HK, Gaebler A, Shevchenko A, Ejsing CS, Thiele C. 2012. Exogenous ether lipids predominantly target mitochondria. PLoS One 7: e31342.
6. Liebisch G, Binder M, Schifferer R, Langmann T, Schulz B, Schmitz G. 2006. High throughput quantification of cholesterol and cholesteryl ester by electrospray ionization tandem mass spectrometry (ESI-MS/MS). Biochim Biophys Acta 1761: 121-128.
7. Liehl P, et al. 2014. Host-cell sensors for Plasmodium activate innate immunity against liver-stage infection. Nat Med 20: 47-53.

8. Niebergall LJ, Jacobs RL, Chaba T, Vance DE. 2011. Phosphatidylcholine protects against steatosis in mice but not non-alcoholic steatohepatitis. Biochim Biophys Acta 1811: 1177-1185.
9. Ploemen IH, et al. 2009. Visualisation and quantitative analysis of the rodent malaria liver stage by real time imaging. PLoS One 4: e7881.
10. Prudencio M, Rodrigues CD, Ataide R, Mota MM. 2008. Dissecting in vitro host cell infection by Plasmodium sporozoites using flow cytometry. Cell Microbiol 10: 218-224.
11. Sampaio JL, Gerl MJ, Klose C, Ejsing CS, Beug H, Simons K, Shevchenko A. 2011. Membrane lipidome of an epithelial cell line. Proc Natl Acad Sci U S A 108: 1903-1907.

Figure S1, related to Figure 1

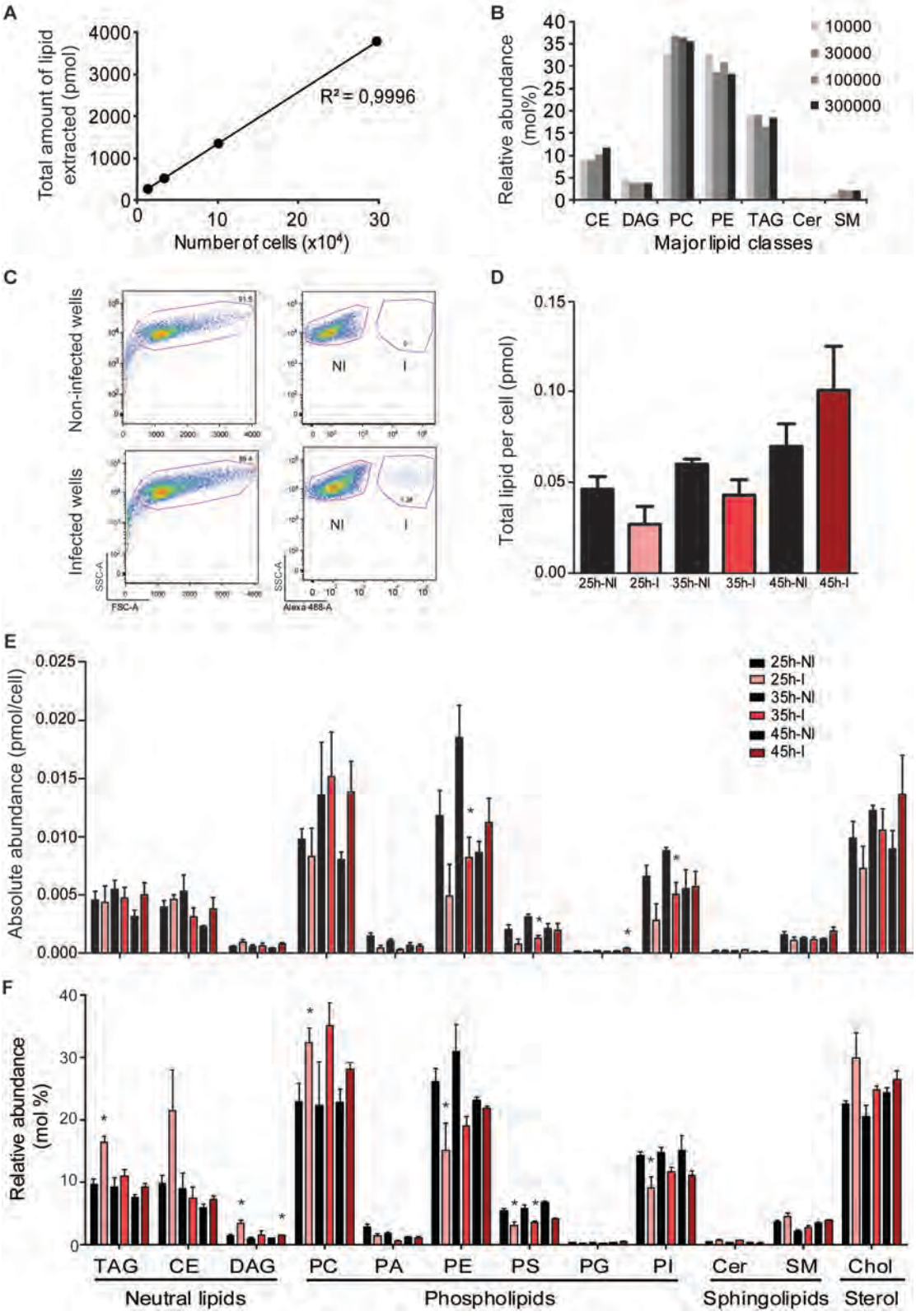

Figure S1. FACS-sorting and lipidomic analyses of *P. berghei*-infected (I) and non-infected (NI) hepatoma cells by shotgun mass spectrometry

(A and B) Determination of the minimum number of Huh7 cells required for optimal quantification of major lipid classes; total cellular lipid was extracted from 10000, 30000, 100000, and 300000 cells including known internal standards and analyzed by shotgun mass spectrometry. Values represent the average of technical duplicates.

(C) Gating strategy to separate *P. berghei*-infected (I) from non-infected (NI) cells by fluorescence activated cell (FACS)-sorting.

(D, E and F) Infected and non-infected cells sorted at 25, 35, and 45 h after infection were subjected to total lipid extraction by Chloroform-methanol technique and extracts were analysed in a LTQ-Orbitrap mass spectrometry instrument. The total lipid per cell is shown in pmol (D), the absolute abundance of major lipid classes normalised per cell in pmol/cell (E), while the relative abundance of major lipid classes is represented in mol% (F). Error bars represent S.E.M. Statistical significance; Unpaired student t-test: * $p < 0.05$, ** $p < 0.001$

Figure S2, related to Figure 1

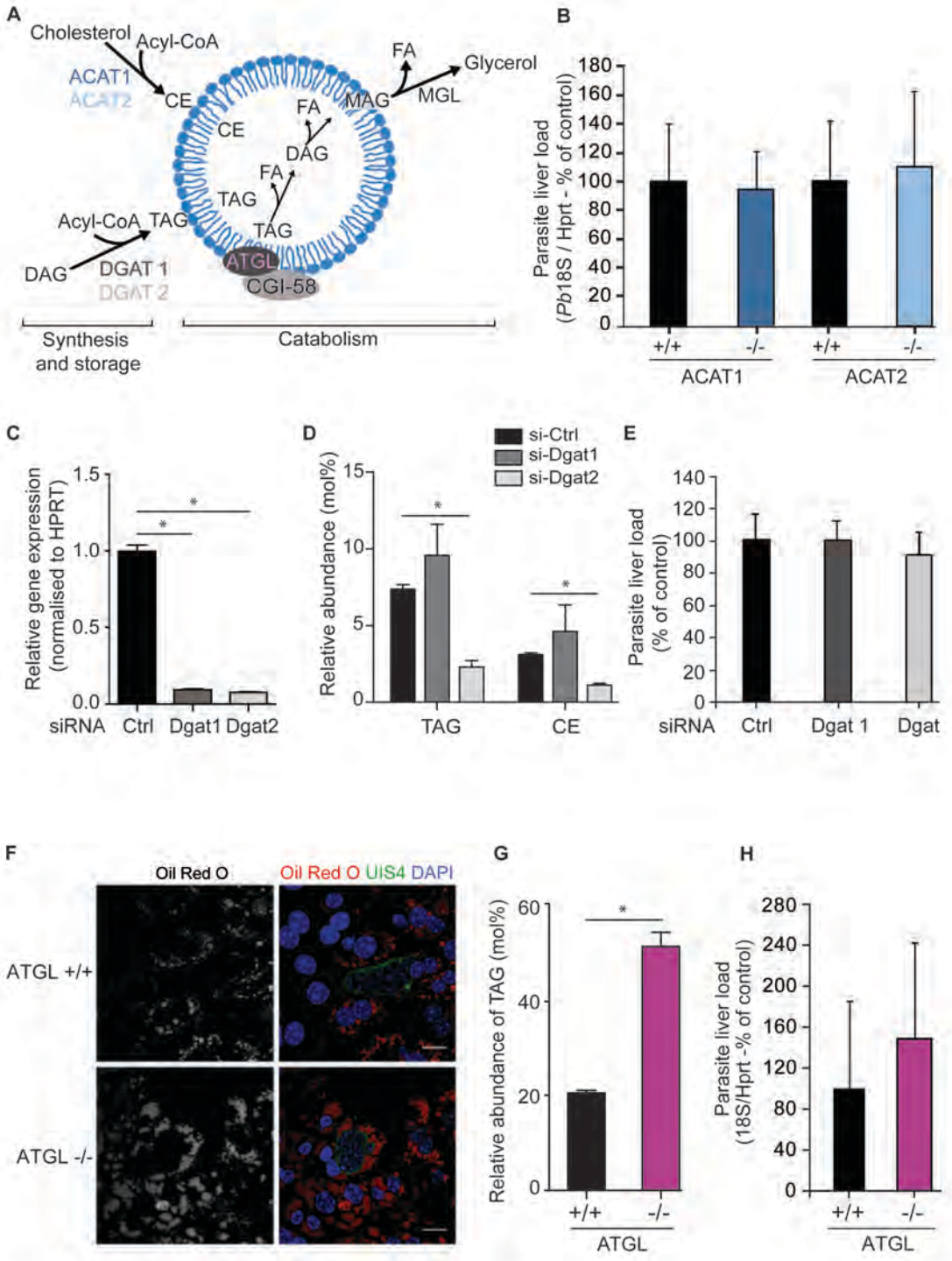

Figure S2. Host cell neutral lipids are not required during *P. berghei* liver stage infection

(A) Schematic representation of the major pathways for neutral lipid synthesis and breakdown. *De novo* synthesized or medium-derived fatty acids are channelled either into the glycerol-3-phosphate pathway to form DAG, which are then converted to TAG by DGAT1 or DGAT2 or conjugated to free cholesterol by acyl-CoA: cholesterol acyltransferase (ACAT1/2) to form CE. The breakdown of TAG, requires the action of ATGL, to remove the first acyl chain from the glycerol backbone.

(B) Mice deficient in ACAT1 or ACAT2 ($ACAT1^{-/-}$ and $ACAT2^{-/-}$) and corresponding wild type controls ($ACAT1^{+/+}$ and $ACAT2^{+/+}$) were infected i.v. with $5x10^4$ *P. berghei* sporozoites and the parasite load in the liver was assessed by qRT-PCR of parasite 18S rRNA 48 h after infection normalised to murine hypoxanthine-guanine phosphoribosyltransferase (HPRT). The data is plotted as percentage of the levels in wild type littermate controls. ACAT1 (+/+ n=5, -/- n=5), ACAT2 (+/+ n=13, -/- n=14)

(C) Huh7 cells were reverse-transfected with control or target specific siRNA to knockdown Dgat1 or Dgat2. Total RNA was extracted from cells and cDNA was synthesized as described in Materials and Methods. The efficiency of the knockdown was assessed by qRT-PCR measurement of the mRNA remaining using primers specific to Dgat1 and Dgat2.

(D) Quantification of the level of TAG and CE by Mass spectrometry after knockdown of Dgat1 and Dgat2. Results represent data from one analysis of technical triplicates for each knockdown and control samples.

(E) 48h after siRNA transfection, cells were infected with luciferase-expressing *P. berghei* sporozoites. The infection level was assessed by measuring luminescence at 48 h after infection and expressed as percentage of control-treated cells. Data is representative of one experiment performed three times.

(F) Primary hepatocytes from wild type ($ATGL^{+/+}$) and ATGL-deficient mice ($ATGL^{-/-}$) were seeded on glass cover-slips and infected with *P. berghei* sporozoites. The cells were fixed with 4% PFA at 48h after infection. Lipid droplets were stained with Oil Red O. Parasite was stained with anti-UIS4 antibodies and nuclei with DAPI. Representative confocal images are shown. Scale bar = 10μm.

(G) Quantification of TAG in primary hepatocytes from $ATGL^{+/+}$ and $ATGL^{-/-}$ mice by mass spectrometry.

(H) Parasite liver load in wild type ($ATGL^{+/+}$) and ATGL-deficient mice ($ATGL^{-/-}$) 48 h after infection with *P. berghei* sporozoites expressed as percentage of levels in wild type. $ATGL^{+/+}$ n=11, $ATGL^{-/-}$ n=10. Error bars represent S.E.M. Statistical significance; Unpaired student t-test: * $p < 0.05$.

Figure S3, related to Figure 2

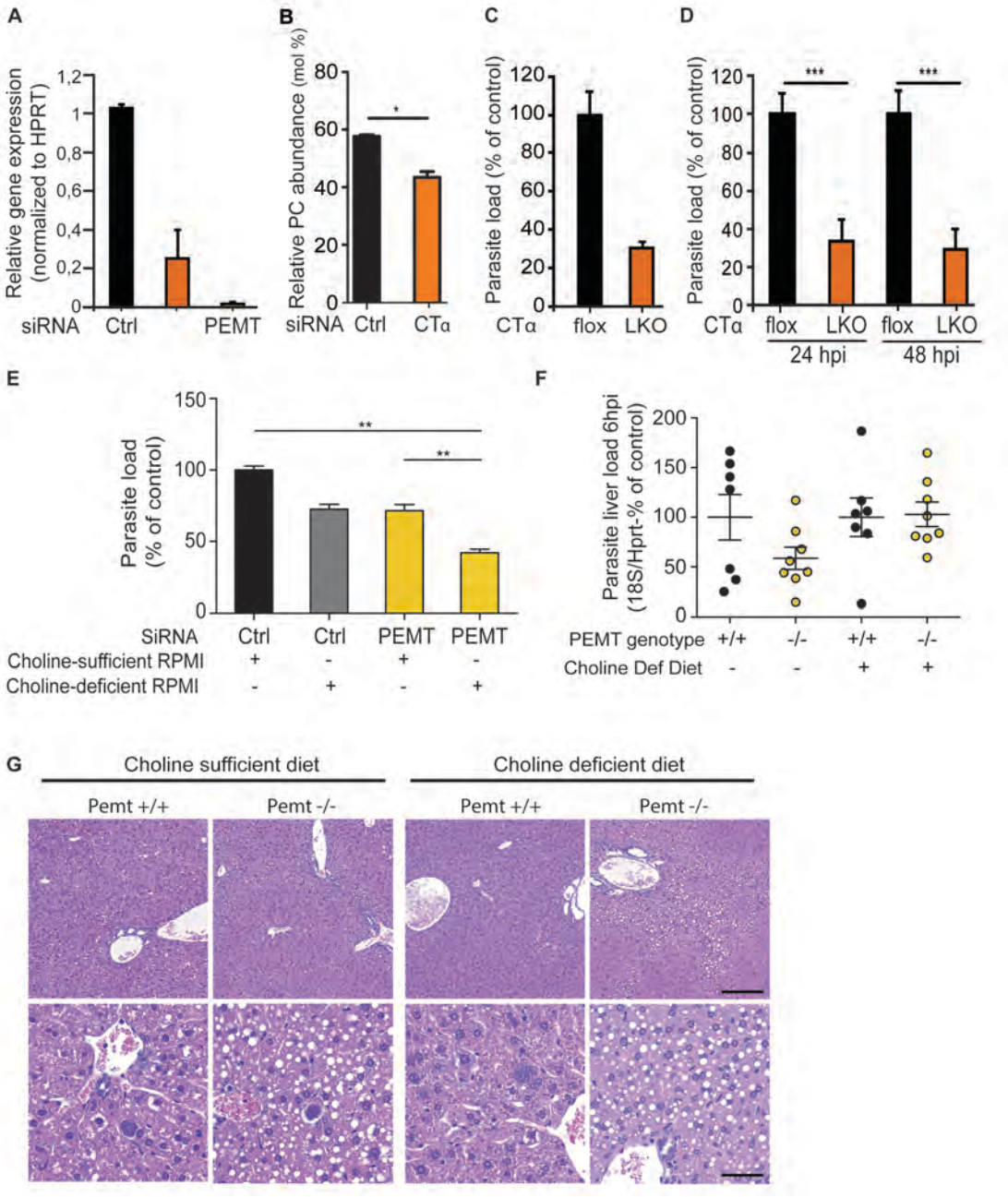

Figure S3. *P. berghei* infection in primary hepatocytes derived from CTα-floxed and CTα-liver-specific knockout mice, and in PEMT-knockdown Huh7 cells and knockout mice on choline-sufficient or choline-deficient conditions.

(A) Huh7 cells were reverse-transfected with siRNA oligonucleotides specific to human CTα, PEMT, or non-specific control for 48 h. Total RNA was extracted from cells and cDNA was synthesized as described in Materials and Methods. The level of mRNA remaining was assessed by RT-PCR using primers specific to human CTα or PEMT.

(B) Primary hepatocytes from livers of CTα-LKO and wild type CTα-floxed mice were infected with luciferase-expressing *P. berghei* sporozoites. Parasite load at 48 h after infection, as determined by luminescence, was plotted as a percentage of control.

(C) *P. berghei* infection in primary hepatocytes from livers of CTα-floxed wild type and CTα-LKO mice, as measured by FACS at 24 and 48 h after infection with GFP-expressing *P. berghei* sporozoites and expressed as a percentage of control. Error bars represent S.E.M. from three independent experiments. Mann Whitney test: *** $p < 0.0001$.

(D) Huh7 cells were reverse-transfected with siRNA oligonucleotides specific to human CTα, PEMT, or non-specific control for 48 h and then infected with *P. berghei* luciferase-expressing sporozoites. One day prior to and during infection for 48 hours, cells were maintained in choline-sufficient complete RPMI 1640 or choline-deficient medium. Parasite load at 48 h after infection was determined by luminescence and plotted as a percentage of control. Error bars are S.E.M. Mann Whitney test: ** $p < 0.001$

(E) PEMT wild type ($PEMT^{+/+}$) and PEMT-deficient mice ($PEMT^{-/-}$) on placebo (n=7, n=8 respectively) or choline-deficient diets for 1.5 days (n=7, n=8 respectively) were infected with $5x10^4$ GFP-expressing *P. berghei* sporozoites and parasite liver load quantified at 6h after infection by RT-PCR of 18S rRNA normalised to HPRT and expressed as percentage of wild type in each condition.

(F) Hematoxylin and Eosin (H&E) staining of Liver sections of *Pemt* wild-type and knockout mice on choline-sufficient and choline-deficient diet. Note the lipidosis in periportal hepatocytes, present in knockout mice on both choline sufficient and deficient diet, although more severe in the later. No hepatocellular necrosis was seen in any of the liver samples analysed and multifocal inflammatory cell infiltrates, of mild to moderate severity, were seen in all groups, regardless of the diet and genetic background. Liver samples from all mice used for parasite quantification were analysed but only representative histological slices are presented. Scale bar = Top panel; 200μm, bottom panel; 50μm. *H&E staining; original magnification: 100x (top panel), 400x (lower panel).*

Figure S4, related to Figure 3

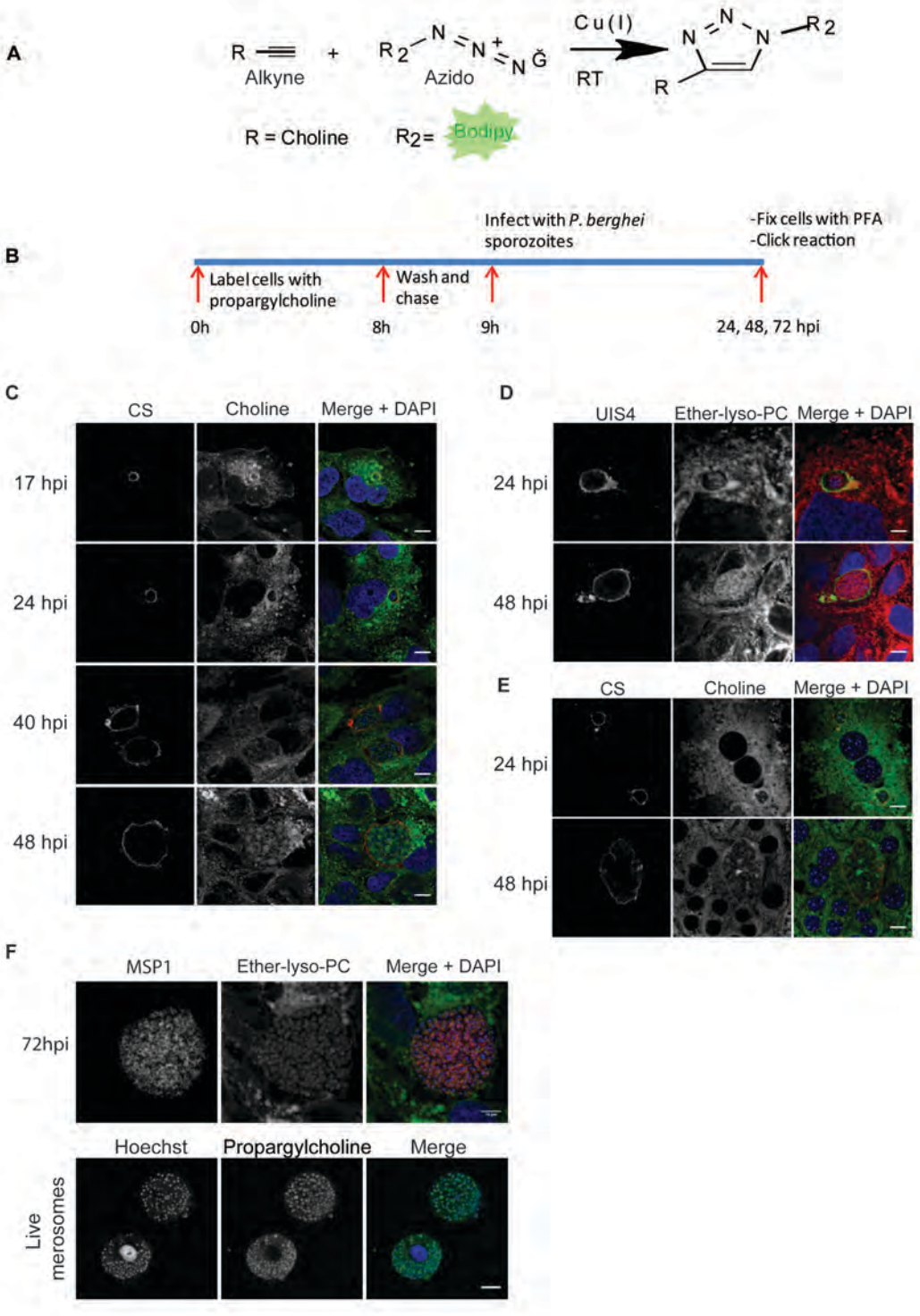

Figure S4. Click detection of choline-containing products/ether-lyso-phosphatidylcholine in hepatoma and primary hepatocytes during *Plasmodium* liver stage infection.

(A) Schematic representation of the cyclo-addition reaction between an alkyne and an azido group catalyzed by Cu^{2+} at room temperature.

(B) Experimental set up for metabolic labeling and *P. berghei* infection

(C) Huh7 cells were pre-labeled with 500 µM of propargylcholine, infected with RFP-expressing *P. berghei* sporozoites and then fixed with 3.7% PFA for 20 minutes at 17, 24, 40, 48 h after infection. Click reaction was performed with an azido-bodipy (green) as described in Materials and Methods. Parasite was stained with mouse anti-CSP antibodies followed by anti-mouse Alexa-Fluor 594 conjugated secondary antibody (red). Nuclei were stained with DAPI (blue).

(D) Huh7 were pre-labeled with 20 µM ether-lyso-PC as in (C), infected with GFP-expressing *P. berghei* sporozoites, and fixed at 24 and 48 hpi. Immuno-staining with anti-UIS4 (green) and Click reaction with azido-TMR (red) were performed as in (C).

(E) Mouse primary hepatocytes were pre-labeled with 500 µM propargylcholine, infected with *P. berghei* sporozoites and fixed at 24 and 48 hpi. Immuno-staining of the parasite with anti-CSP and Click reaction with azido-bodipy (green) were performed as in (C). Scale bar = 10µm.

(F) HepG2 cells were infected with RFP-expressing *P. berghei* sporozoites, fixed at 72 hpi and immuno-stained with anti-MSP1 (red), DAPI (blue), followed by click-labeling with azido-bodipy as in (A) and (B) (top panel). Detached merosomes from HepG2 cells were click-labeled and imaged by live confocal fluorescence microscopy (lower panel). Scale bar= 10µm.

Table S1. Lipidomics raw data, related to Figure 1

	Non-infected (NI)					Infected (I)		
Lipids	25h_NI-1	25h_NI-2	25h_NI-3	25h_NI-4	25h_NI-5	25h_I-1	25h_I-2	25h_I-3
CE 14:0	0,289852498	0,182668681	0,284813732	0,395897166	0,191243012	0,804102978	0,628612632	0,258000848
CE 14:1	0,05185574	0,030499456	0,048349336	0,065125958	0,037571361		0,145963075	0,038046478
CE 15:0	0,048229748	0,027091921	0,047188374	0,091938635	0,049617247	0,419263708	0,263910232	0,106661962
CE 16:0	0,998194491	0,596495062	1,025974966	1,515905382	0,808585941	6,26795944	2,718056695	1,320508027
CE 16:1	1,195968523	0,76237639	1,201426025	1,620457753	1,01107724	3,81970839	2,715012773	1,363156152
CE 16:2	0,07114144	0,057677944	0,072916382	0,064886553	0,042258554	0,055447997	0,083645888	0,043995983
CE 17:1	0,148075586	0,075241307	0,134973857	0,211629205	0,146939446	1,172589388	0,443292427	0,250734785
CE 18:0	0,181854763	0,113582023	0,173157145	0,261558284	0,147599508	0,865460445	0,437077344	0,214478044
CE 18:1	3,32991329	2,499222291	3,554946535	4,738476544	3,010555227	11,20554042	6,843458683	3,980393481
CE 18:2	0,631033292	0,442738346	0,690511041	0,801390633	0,504775597	3,082961581	1,299642504	0,676763042
CE 18:3	0,079442878	0,047141018	0,091356342	0,095077249	0,0702791	0,398916148	0,151255461	0,091168877
CE 19:1	0,110765237	0,054268223	0,096572557	0,13253191	0,080366285	0,201729973	0,196462662	0,103879215
CE 19:2	0,049974467	0,030694957	0,049789541	0,058095081	0,039427757	0,02986998	0,045524374	0,037424577
CE 20:1	0,130498733	0,112489032	0,138060566	0,180201217	0,106468826	0,183080047	0,230260036	0,137918164
CE 20:2	0,168634581	0,132594053	0,161273048	0,18080144	0,116107172	0,21751181	0,216111203	0,146151473
CE 20:3	0,271017391	0,154127888	0,25294692	0,295673098	0,290685484	0,593435559	0,388509254	0,309686694
CE 20:4	0,21248214	0,089347151	0,192057509	0,312655337	0,328003614	2,272666684	0,664958117	0,445087674
CE 20:5	0,14122052	0,042622284	0,091584194	0,188424855		0,651406511	0,301602586	0,588801044
CE 22:3	0,054035417	0,03672785	0,051534785	0,044847161	0,030091726	0,018322739	0,031679348	0,01909504
CE 22:4	0,048882437	0,022803297	0,03137714	0,051842866	0,057415357		0,043729863	0,056513907
CE 22:5	0,157614125	0,057800258	0,093439877	0,187266456	0,389089274	0,163752006	0,236862853	0,357790973
CE 22:6	0,920248649	0,481004157	0,578675597	0,986420589	1,108743856	1,186070693	1,219127067	1,123110538

PG 34:2	0,029495045	0,037108678	0,042574024	0,034700755	0,043977109		0,022570453	0,041021216	0,033615483	0,037051507	0,02236923	0,023529156	0,016891571	0,027473754	0,042642141	0,043378037	0,051365307	0,050449771	0,025146312	0,029011988	0,029939491	0,028307437			0,046634555	0,04744153	0,037738327	0,038034234
PG 34:3	0,001932687	0,001721863	0,004236053	0,002865251	0,0105596				0,003803246	0,008111504	0,003719269				0,009051014	0,005614771		0,003476877	0,001325094	0,002113234	0,002606593	0,001207236	0,009382759	0,007672364				0,001463041
PG 36:1	0,019007179	0,024474512	0,016011157	0,013777236	0,020744142		0,011366342	0,019146541	0,024502571	0,016803075	0,018016061	0,030416766	0,018515969	0,039938028	0,027918113	0,025931553	0,031390255	0,019394883	0,027260326	0,028769548	0,029499478	0,034027063	0,104374125	0,100764242	0,079202608	0,084863782	0,054397004	0,052580006
PG 36:2	0,03655077	0,060201086	0,058183364	0,04554295	0,033682296	0,01388811	0,033351748	0,034992224	0,046591437	0,028878716	0,034312134	0,045014088	0,029870624	0,048367381	0,086433425	0,091153552	0,090672449	0,090976413	0,059418929	0,060494887	0,063795619	0,058114049			0,167004472	0,169244079	0,115907101	0,109556008
PG 36:3	0,007302307	0,014824044	0,020159205	0,01433118	0,011691673	0,012222406	0,004427439	0,006564242	0,005850452	0,007278245	0,007229		0,010264989	0,004221697	0,030931415	0,03114639	0,031061612	0,032539185	0,015706075	0,016547015	0,014218647	0,016793284			0,032074361	0,028523963	0,024232644	0,025130785
PG 36:4			0,001863402		0,002666433		0,0031474	0,004267678	0,002313185	0,002253194	0,002340114	0,004192511	0,006928748	0,007640263	0,004410553	0,001569324		0,001395288	0,001365222		0,001490689				0,026334005	0,01786353	0,011745408	0,009017098
PG 38:3															0,009450047	0,00635178	0,008629847	0,00770742	0,003789318	0,001888417	0,002875018	0,002327809			0,012973955	0,006735592	0,002406637	0,005512957
PG 38:4	0,001904523	0,002307351	0,00243924	0,001783495	0,001272321		0,005158318	0,00454632				0,021002725	0,024288742	0,02860413	0,009994731	0,006166428	0,004913967	0,003427645	0,005231056	0,005657925	0,002706057	0,004082745	0,075554886	0,075181941	0,064930119	0,072080053	0,045051312	0,041170335
PG 38:5															0,007805845	0,003362495			0,00412137	0,001619928	0,00243484	0,001707037	0,081494862	0,085148489	0,055954118	0,059688067	0,03474244	0,033121248
PG 38:6	0,008112629	0,00551208	0,012124994	0,008072919	0,007974638	0,085767794	0,006298576	0,007439989	0,005241142	0,00424108	0,004376984		0,005468158	0,008136099	0,015164553	0,013939458	0,015134056	0,01637671	0,007306911	0,006523305	0,004041035	0,00519477			0,013255989	0,011010565	0,007436853	0,008429732
PG 38:7	0,011560217	0,010861012	0,020454319	0,012931497	0,007024772		0,003883423		0,00867435	0,006746619	0,005481101				0,023814831	0,02495263	0,028124097	0,031799618	0,01285955	0,012732334	0,010746731	0,012212849	0,007711973	0,007713177			0,002615106	0,003768038
PG 40:7	0,08756076	0,112499253	0,125753959	0,103846372	0,066292679	0,012191411	0,082236544	0,058475142	0,069623798	0,066126222	0,06283837	0,030844959	0,013115806	0,027727035														
PG 40:8	0,013803519	0,012915647	0,028007805	0,014826487	0,011133603		0,004078778	0,004401848	0,016645613	0,009333927	0,007731442				0,027953852	0,028974358	0,037104478	0,036316574	0,016424306	0,014752194	0,015359931	0,014097793	0,011117866	0,008879203	0,005916119	0,00546673	0,004617415	0,008241345
PI 32:1															0,071482317	0,065097581	0,068915842	0,063662179	0,038381888	0,037176816	0,016666537	0,021825268	0,06083795	0,065286211	0,01468118	0,014456399	0,007176581	0,005252466
PI 34:1	0,129216498	0,132272185	0,125795911	0,131616698	0,035544977	0,030233881	0,107996181	0,068853792	0,034741651	0,106414896	0,136670925	0,127492926	0,100986741	0,07136535	0,303342498	0,296070269	0,315813325	0,292257649	0,22994937	0,246930111	0,141701113	0,142032491	0,376244353	0,32160897	0,14737242	0,144189622	0,124801755	0,111173034
PI 34:2	0,312519473	0,314236855	0,263457873	0,240004995	0,126455899	0,042601694	0,155020932	0,105340316	0,092510938	0,150207806	0,193887726	0,158732502	0,12825008	0,092701147	0,4945622	0,435201289	0,548986604	0,478988603	0,326067065	0,323762872	0,264551696	0,274980414	0,54121624	0,511630892	0,169685043	0,174199636	0,171897967	0,15930594
PI 34:3	0,036925146	0,063571374	0,0412083	0,021294771	0,003613104		0,006445531		0,00022237	0,006524436	0,011586404				0,092984022	0,078141526	0,095788734	0,078130117	0,059051095	0,058092239	0,051366993	0,055931833	0,066350833	0,062391828	0,007888435	0,016422561	0,025940625	0,015372843
PI 36:2	0,396618319	0,428683319	0,291516187	0,351535533	0,187938052	0,021249109	0,214169165	0,165997421	0,289386922	0,277113835	0,265989933	0,236710569	0,206888402	0,194450059	0,619247134	0,598285049	0,690016795	0,600680663	0,471519029	0,470772327	0,346298062	0,338502712	0,872601361	0,888077256	0,383736156	0,383848813	0,343627084	0,332560511
PI 36:3	0,836253369	1,875231939	1,132816708	0,779216855	0,221789911	0,58476364	0,424111338	0,194439247	0,050948593	0,34203865	0,31109032	0,190070292	0,302615417	0,193746093	0,900502063	0,848154782	1,023425711	0,90378387	2,02712	1,892286695	1,907714988	1,923088882	0,704384435	0,660109691	0,583794362	0,572454507	0,82053768	0,76644436
PI 36:4	0,91801058	0,586339852	0,621640023	0,759704946	1,295059725	0,197508293	0,499595521	0,845127886	1,957541446	1,547850628	1,397874157	0,91807343	0,698316511	0,784095106	0,837249726	0,742698059	0,781333059	0,711572722	0,797391524	0,747171295	0,726704484	0,741827826	0,523197399	0,478466273	0,459547543	0,477375227	0,503527395	0,415322048
PI 36:5	0,068949039	0,046624129	0,043551008	0,052167547	0,067530748		0,01624025	0,047523766	0,10312167	0,099780727	0,079244189	0,031820685	0,014566262	0,032826084														
PI 37:3	0,081745124	0,11831658	0,102112952	0,093046114	0,087166644		0,053052512	0,068798003	0,037972044	0,07379418	0,077959749	0,007882321	0,016240526	0,035037374	0,129540542	0,126405942	0,134925286	0,119138359	0,110249141	0,113668927	0,091427145	0,091393959	0,096217247	0,090317715	0,072161183	0,073431783	0,06201829	0,06016262
PI 37:4	0,058864758	0,05627101	0,035652914	0,049834314	0,085813273		0,017977281	0,076451424	0,117397042	0,100379149	0,078951756	0,050214425	0,025844791	0,052320521	0,095792449	0,089187849	0,081703883	0,073919714	0,054170788	0,054496944	0,050020553	0,046887417	0,064410507	0,05892565	0,02746069	0,029867464	0,031023343	0,028959946
PI 38:3	1,92191313	4,737977934	3,673745468	2,028522506	0,199216069	0,865143526	0,740524872						0,131916646		1,529628581	1,563836897	2,429456954	1,687467876	5,60417167	5,320174466	4,610620896	4,613663616	1,28224249	1,546417098	2,015604759	2,049112541	2,247959913	2,457886946
PI 38:4	7,219504556	6,189637199	6,287208857	6,672347671	9,991503433	1,91535961	5,088317978	9,175896522	10,3448785	9,30331872	8,357720795	9,034175403	6,870522715	7,96052338	3,911241835	3,741303403		3,329803136	7,841801663	7,560245311	6,995641397	6,94724021	2,965250307	2,859178922	6,220140128	6,444488957	5,667127282	5,350449287
PI 38:5	1,766422292	1,271306897	1,035631713	1,227507005	1,234816348	0,386870731	0,732426464	0,830942209	2,018834396	1,537170128	1,400519575	0,910169825	0,729672052	0,881602531	1,463308505	1,307521046	1,197239502	1,098397682	1,551860817	1,461302072	1,421909148	1,490683975	1,004473182	0,924438567	1,019058115	0,985631076	1,051377256	0,968323218
PI 38:6	0,194312614	0,202167308	0,141667489	0,152793759	0,115335172		0,085558834	0,088732749	0,172653138	0,214381206	0,187175912	0,064957183	0,063833295	0,086806937	0,188882445	0,176276697	0,238542201	0,21243933	0,15089366	0,161643076	0,170793788	0,162610546	0,172389598	0,148630139	0,110700364	0,111901266	0,136223541	0,10966389
PI 40:3	0,242436341	0,34176249	0,340908794	0,336575463	0,20152098	1,949633126	0,504909017	0,294003759	0,209545206	0,249487672	0,230054426	0,72899141	0,635072944	0,418606441														
PI 40:4	0,050571921	0,084550495	0,04810677	0,042936318	0,020951926	0,075895222	0,034797556	0,017293298	0,01823858	0,012896928	0,021710299	0,051574056	0,034973308	0,037131423	0,079967313	0,081827254	0,094121485	0,078131309	0,065086338	0,062507299	0,064029674	0,057704104	0,181190385	0,168222272	0,093444276	0,083542759	0,083963942	0,079030302
PI 40:5															0,081361434	0,078255398	0,068054204	0,062959138	0,032820548	0,028579661	0,025835128	0,037004453	0,119817287	0,114844057	0,050087816	0,040222307	0,042753177	0,038577343
PI 40:6	0,211690371	0,246206608	0,179036153	0,189762214	0,144359455	0,022771882	0,134863806	0,124659841	0,106480244	0,156430137	0,175429381	0,231272188	0,266090899	0,256834738	0,195077947	0,198074556	0,262953113	0,242085966	0,208368582	0,217017676	0,17845166	0,170469624	0,517724703	0,480624859	0,288558129	0,296821592	0,22948404	0,204790718
PI 40:7	0,219478307	0,20766352	0,148674172	0,212011867	0,194262686	0,022463631	0,146226313	0,175545904	0,436851927	0,605054359	0,243827119	0,357866516	0,307806176	0,278741055	0,127561709	0,133220047	0,16317495	0,155894721	0,143348467	0,157372896	0,163416029	0,158166076	0,172843702	0,158335906	0,211198474	0,212933944	0,171035634	0,147651694
PI 40:8	0,050548017	0,032992019	0,020498743	0,042725094	0,028270933		0,010140483	0,012064542	0,089598314	0,115566183	0,064072976	0,027640808	0,019309762	0,028791044														
PS 32:1	0,1542368	0,176573763	0,143898039	0,137885396	0,049722581	0,023813449	0,126563124	0,069128414	0,061547071	0,070919067	0,068711516	0,066839025	0,091567249	0,079741487	0,335393646	0,283474301	0,342259933	0,299839855	0,126584405	0,118943874	0,152261732	0,15803478	0,336853682	0,322020775	0,122263668	0,124070682	0,148259082	0,134383431
PS 34:1	0,951077768	1,022167484	0,713244186	0,757886219	0,516834867	0,303164753	0,598642333	0,50301923	0,547956331	0,589385309	0,467847753	0,496642079	0,538326916	0,509298437	1,230469817	1,129723524	1,354446214	1,198233738	1,054078531	1,005992589	1,105774884	1,158661613	1,081929022	1,048477548	0,74836997	0,733143366	0,866136498	0,842724429
PS 34:2	0,138510653	0,197181739	0,140602766	0,119750749	0,073016416		0,079943592	0,069964413	0,082258694	0,08136324	0,072010018	0,061648497	0,052651535	0,07202314	0,293736155	0,250595195	0,318897986	0,298342332	0,142294808	0,14599434	0,167492582	0,161481632	0,227466307	0,221789046	0,09880959	0,10635767	0,119136241	0,103507851
PS 35:1	0,01701107	0,005637012	0,008790374	0,00566202	0,019217204		0,003646167	0,025478894	0,024571868	0,058211894	0,010941329	0,041159468	0,008927847	0,013067038		0,031643126	0,04938935	0,087483499	0,029255201	0,026326073	0,010782123	0,009664716			0,005991377		0,012494167	0,006151842
PS 36:1	0,560845692	0,669740881	0,430060107	0,478470318	0,659842575	0,228030168	0,393105124	0,591351814	0,51704675	0,487115047	0,419233002	0,50273341	0,498919815	0,483131308	0,76478583	0,76287463		0,821222636	0,824804322	0,793126208	0,743692245	0,769598501	0,750768108	0,697164154	0,687685003	0,709669509	0,684558973	0,703917664
PS 36:2	0,46436861	0,607065407	0,475257033	0,429565425	0,573310279	0,138118966	0,279113462	0,392429266	0,691350951	0,531435616	0,468015757	0,428197387	0,360782592	0,339447504	0,808340086	0,743997385	1,074195954	0,965401568	0,722781987	0,688074035	0,739812684	0,773399888	0,559748927	0,55943285	0,399663101	0,396678468	0,48526941	0,446805851
PS 36:3	0,120649244	0,162484337	0,145241537	0,122769704	0,064362405	0,49184814	0,149457412	0,096924649	0,088235703	0,10845853	0,084387377	0,181935804	0,193684272	0,107110159														
PS 36:4	0,106168516	0,088805588	0,084268061	0,085680978	0,063818675		0,069351632	0,075434767	0,08384458	0,117734234	0,069135936	0,080291312	0,079870119	0,097463956	0,173133839	0,165105239	0,169796188	0,161866873	0,068608894	0,078296312	0,104627519	0,101347539	0,127935423	0,105735214	0,100757412	0,103894148	0,098233299	0,085128645
PS 37:1	0,083963553	0,102231315	0,103321596	0,084782982	0,078481527		0,069330403	0,064360363	0,057259783	0,180716804	0,057141771	0,152152051	0,049628532	0,057021465	0,059886927	0,091270695	0,097618861	0,095046737	0,059645253	0,060212906	0,052630307	0,052038614	0,090625959	0,074507452	0,045232569	0,043365126	0,032428624	0,033319353
PS 37:2	0,00725754	0,006215955	0,006238309	0,007033061	0,008868357			0,003432902	0,005139197	0,033240283	0,002789706	0,021251259	0,007941875	0,004256607														
PS 37:3	0,007600942	0,006591176	0,003131237	0,005268691	0,011834897			0,004661754	0,00899632	0,012671359	0,008303551																	
PS 37:4	0,003575846	0,003051092	0,002290884	0,002284657	0,015138058			0,006103616	0,027043909	0,01582484	0,012833799	0,001655289		0,004462132														
PS 38:1	0,031597913	0,040976569	0,033579541	0,033303343	0,030027697		0,012008455	0,015157475	0,023434555	0,024008681	0,0184829	0,015975857	0,00854243	0,007017072	0,036332498	0,046631183	0,053632522	0,049921561	0,040111201	0,036490562	0,010582325	0,01218052	0,043355259	0,052559103	0,016565594	0,006918646	0,011988044	0,019492916
PS 38:3	0,479662513	0,588007658	0,525570665	0,410632024	0,432060295	0,16909922	0,251629575	0,254770953	0,358410451	0,386545131	0,354625966	0,185314109	0,21569341	0,209216174	0,557810177	0,545713704		0,601188324	0,770632074	0,734477469	0,83393682	0,843246425	0,208890549	0,23864966	0,308707312	0,314666948	0,420344324	0,407967311
PS 38:4	1,006911263	1,10341335	1,064767225	1,055479557	2,20531003	0,343134152	0,57797224	1,235437676	2,387281611	1,944660251	1,652043062	0,891529273	0,731660825	0,879931193	1,306149725	1,206737478	1,158029755	1,024963214	1,468806758	1,350323639	1,602162918	1,664645366	0,41224794	0,394528989	0,717399183	0,725422812	0,894554257	0,812226766
PS 38:5	0,251319072	0,235466687	0,204104981	0,204490414	0,497714079	0,081246961	0,14375982	0,289733666	0,383422373	0,380873139	0,321376381	0,212241887	0,196772686	0,200739062	0,312651689	0,279458365	0,326720067	0,312061803	0,148939277	0,15928247	0,234179037	0,227557426	0,15149457	0,123709022	0,157078082	0,15962943	0,178599947	0,151197234
PS 38:6	0,061375476	0,041898159	0,043517708	0,047734978	0,041597515		0,023895385	0,030042219	0,043353871	0,039725377	0,034461967	0,011974434	0,010469014	0,022510831	0,105790514	0,096814309	0,10714955	0,106776931	0,020417905	0,014534109	0,048475159	0,045149107	0,069997989	0,065981291	0,027843152	0,025091621	0,039090202	0,038035353
PS 39:1	0,053968296	0,081244627	0,071895208	0,059332564	0,046484967		0,060718581	0,030515796	0,032887254	0,087554867	0,03298082	0,06596254	0,018878062	0,029123866	0,040945434	0,072087857	0,071997436	0,062716007	0,048214648	0,049199914	0,042532367	0,041016836	0,072465298	0,058474195	0,029804359	0,031008956	0,023025921	0,019223135
PS 39:2	0,0115061	0,03123359	0,028546201	0,015536559	0,012925231		0,004545633	0,006677796	0,003924209	0,033199272	0,004510103	0,041496085		0,014137219														
PS 39:3	0,017675563	0,014858602	0,017836177	0,015372013	0,03607146		0,004472023	0,019439819	0,027211709	0,059236591	0,021845736	0,047680464	0,012631022	0,01096664														
PS 39:4	0,004734586	0,003759032	0,004584079	0,004092085	0,017366318			0,010453237	0,010970145	0,029741018	0,007772766	0,040681379																
PS 39:5	0,014343009	0,006501794	0,015709073	0,021657836	0,012333578	0,12577974	0,022393237	0,018654213	0,016431873	0,04838731	0,006440561	0,127297126	0,040471334	0,009534869														
PS 40:1															0,010720736	0,024145678	0,007430101	0,025495272	0,009586694	0,013995563	0,004467352	0,005650092	0,00581968	0,01079639	0,006566764			0,003372042
PS 40:2															0,018099257	0,021838228	0,032723244	0,028594796	0,010255203	0,008790915	0,008873564	0,007822412	0,022113233	0,024478178	0,004992566	0,004801103	0,006250794	0,00727595
PS 40:3	0,01289925	0,017368745	0,01274554	0,011157167	0,017250051		0,004165289	0,006634342	0,008898413	0,003439588	0,004313676			0,006103734	0,034492226	0,03643156	0,032889135	0,037024344	0,012030964	0,01777983	0,01004141	0,011192564		0,013142681	0,006480418	0,005992839	0,006503471	0,00840883
PS 40:6	0,655903113	0,536991733	0,39797924	0,50806016	0,564395061	0,068440668	0,189061678	0,188471656	0,905349906	0,49989414	0,455105144	0,212218346	0,155312179	0,183967164	1,129278224	1,058525526	0,787061563	0,712901411	0,656884928	0,58547569	0,82345498	0,845186669		0,056336528	0,176925259	0,188591202	0,363198812	0,325123461
PS 40:7	0,093745252	0,077122278	0,064359339	0,085221941	0,101343835		0,034650404	0,06596162	0,167219514	0,237899357	0,09742855	0,078723502	0,056850244	0,062180503	0,172067366	0,168118028	0,139599808	0,145738661	0,074289089	0,074308722	0,115540124	0,09924111	0,054110112	0,044244326	0,086027735	0,092469124	0,085571471	0,0779042
PS 40:8	0,010861134	0,007519818	0,005833861	0,010633218	0,025392691			0,009217268	0,030394863	0,057735723	0,012446331	0,005717099		0,001983978	0,007391766	0,019353316	0,014129442	0,022418397	0,006062085	0,006199004	0,008493932	0,008229354		0,003568917	0,003134471	0,004748507	0,003696388	0,003208906
Cer 32:1:2	0,00305722	0,003015749	0,003488689	0,002893355	0,003981782	0,001641238	0,00400581	0,004179716	0,003099784	0,003637732	0,002667621	0,003633351	0,004809352	0,003275047														
Cer 33:1:2	0,001648801	0,001063344	0,001373114	0,001638384	0,003340251		0,002284566	0,004256821	0,002571228	0,00229464	0,001973438	0,002508636	0,002844566	0,002465114														
Cer 34:0:2	0,00369461	0,00258483	0,002194108	0,003715805	0,01046592	0,005666654	0,006794573	0,016666911	0,004850742	0,006809545	0,003325827	0,0097516	0,01839555	0,006871622														
Cer 34:1:2	0,066659883	0,061468499	0,066104014	0,065705429	0,095170888	0,059206039	0,086929676	0,130136793	0,065434204	0,067449713	0,052424003	0,080595849	0,097905134	0,074140008	0,06300207	0,07954976	0,077913756	0,066404755	0,049322898	0,051842867	0,03015219	0,032347207	0,067352692	0,08978673	0,056728365	0,050870138	0,035776244	0,033938384
Cer 34:2:2	0,002891298	0,003090788	0,004047084	0,003495024	0,004468376	0,001084925	0,004413939	0,004072255	0,003700978	0,004158914	0,003113996	0,002550998	0,0043071	0,002824923														
Cer 36:1:2	0,008204377	0,006671503	0,008526631	0,008799431	0,013224028	0,03141957	0,017971921	0,023880303	0,010582329	0,013576983	0,009340902	0,025398993	0,049072016	0,025911617														
Cer 36:2:2	0,001648145	0,001511502	0,002130635	0,001957405	0,002304832	0,002061995	0,003026098	0,003087963	0,002135942	0,003358489	0,002063263	0,00257449	0,005377383	0,002893473														
Cer 38:1:2	0,009057766	0,008731601	0,014723396	0,017198579	0,010574211	0,160099395	0,04380155	0,077815281	0,013228104	0,011971488	0,020517295	0,072008905	0,164725193	0,088173413														
Cer 38:2:2	0,001009981	0,001191771	0,001598866	0,001471221	0,001468485	0,001365054	0,002635296	0,002812856	0,001464066	0,00180996	0,002665381	0,003178266	0,006126159	0,004941982														
Cer 39:1:2	0,001298067	0,000799614	0,001213215	0,001333552	0,002081466	0,004744764	0,003237964	0,00420939	0,001788823	0,001514114	0,001572531	0,004695992	0,006155023	0,004703696														
Cer 40:1:2	0,038235278	0,035626756	0,046385972	0,052876973	0,042613019	0,31579104	0,105289635	0,131551999	0,037645764	0,034266804	0,038083168	0,13824078	0,203042895	0,149689331	0,027625798	0,033232488	0,032746982	0,028888265					0,04082172	0,042854439				
Cer 40:2:2	0,013299837	0,016614351	0,017773195	0,015563894	0,017777323	0,026836031	0,019975914	0,024580733	0,01049525	0,011722962	0,01429314	0,020517388	0,027770088	0,025245632		0,023352005	0,025793234	0,02209736	0,010848137	0,010735452	0,013405598	0,013727281	0,058470231	0,050411554	0,019435681	0,019039366	0,020056262	0,019885259
Cer 41:1:2	0,007409766	0,004488714	0,005728551	0,006681136	0,010043894	0,010044429	0,0099147	0,011806037	0,008117079	0,007027641	0,005776968	0,010329061	0,009870188	0,007505501	0,001821121	0,003348584	0,002459133	0,002990172	0,003160205	0,003140176	0,002669167	0,003023091	0,000693639	0,001414077	0,004302886	0,004299948	0,003459931	0,003171348
Cer 41:2:2	0,004319358	0,003398448	0,004167206	0,004393426	0,008306648	0,000904822	0,005517693	0,008623548	0,004435059	0,00391638	0,003158746	0,005234597	0,004806678	0,004617782														
Cer 42:0:2	0,002190075	0,000912193	0,001070973	0,003097753	0,002543214	0,00964206	0,006088442	0,005763596	0,003739461	0,004399878	0,002541087	0,006582301	0,0070876	0,003398704														
Cer 42:0:3	0,002283537	0,001113376	0,001521751	0,002012148	0,000524713	0,023394464	0,00664276	0,004645597	0,000867036	0,000946212	0,001298974	0,002813316	0,004373795	0,001698426														
Cer 42:1:2	0,104680692	0,099667003	0,097961323	0,111803319	0,084498197	0,072633564	0,107389763	0,081570957	0,078620639	0,079172186	0,056500007	0,09242513	0,076531426	0,062021887	0,073420687	0,08140211	0,074041938	0,065185977	0,094441275	0,089015491	0,080449649	0,079063525	0,043468109	0,046098377	0,082743389	0,074045992	0,065968624	0,064641108
Cer 42:1:3	0,00404199	0,001390507	0,001422169	0,001814226	0,000943766	0,023857849	0,007951169	0,0053702	0,000937439	0,000998449	0,001734255	0,003146573	0,004974147	0,001917276														
Cer 42:2:2	0,123224219	0,129914824	0,133416233	0,131686569	0,12077705	0,070130073	0,131014148	0,123769136	0,077183123	0,079942133	0,061031739	0,083699616	0,070879131	0,071215145	0,13031221	0,136791705	0,140535224	0,122635202	0,117255958	0,107086899	0,094748933	0,093008115	0,10889404	0,105643947	0,120274304	0,10972717	0,091263775	0,089886337
Cer 42:3:2	0,019006942	0,024331064	0,026686259	0,021030225	0,021113051	0,014257899	0,019423689	0,017341929	0,010473453	0,009933955	0,008725563	0,008994131	0,008338062	0,008859223														
Cer 43:1:2	0,00405092	0,002484284	0,002841923	0,003800783	0,004262091	0,006392863	0,005810414	0,005455013	0,004614188	0,003995845	0,003269034	0,005083915	0,004543668	0,003029959	0,000253418	0,000589651	0,000801842	0,000443842	0,002004673	0,001885281	0,001503394	0,001351102			0,002751658	0,001937021	0,001117976	0,001150682
Cer 43:2:2	0,003548835	0,002900384	0,003192744	0,003627365	0,005905455		0,00362328	0,005743172	0,003968952	0,003903875	0,002805246	0,003935388	0,002716355	0,003023744	0,000766528	0,001414913	0,000903091	0,001330164	0,001985916	0,001940043	0,001119634	0,000976327			0,002357136	0,001686294	0,000963086	0,000600804
Cer 44:1:2	0,004476679	0,002674879	0,002616012	0,003369356	0,00169265	0,012511857	0,006862915	0,004537801	0,002182545	0,002272242	0,001934262	0,00368718	0,004987387	0,002411235														
Cer 44:1:3	0,00279103	0,000849438	0,001178815	0,00132588	0,000237854	0,025573595	0,007915382	0,005331069	0,000481155	0,000570936	0,001453375	0,002651532	0,005182906	0,001523735														
Cer 44:2:2	0,005274298	0,007141289	0,005866219	0,005682187	0,003554416		0,004560603	0,002842039	0,002630312	0,003041578	0,002045783	0,002829658	0,002122961	0,002206579	0,003828527	0,007342699	0,004754645	0,005365369	0,004174255	0,004074584	0,004400268	0,004039918	0,001745573	0,001491783	0,003698866	0,003388593	0,003603073	0,003109074
SM 33:1;2	0,069645142	0,05500495	0,065345759	0,077014579	0,114850026	0,112020624	0,087285841	0,09177892	0,07154981	0,058748717	0,057832213	0,090292667	0,054690991	0,063087954	0,083089828	0,081624018	0,095267615	0,085438647	0,052109057	0,051352059	0,047989725	0,047787499	0,07900938	0,074796049	0,057593745	0,05602186	0,057033433	0,0617135
SM 34:0;2	0,146939475	0,110082434	0,116678268	0,151147983	0,252612247	0,178475751	0,169650034	0,233260021	0,151415438	0,154012855	0,086565294	0,247541675	0,158172938	0,122767868	0,096303964	0,102560251	0,105612464	0,089329893	0,082510354	0,084194614	0,093001238	0,090529231	0,148944093	0,14232562	0,117936434	0,116300121	0,114574552	0,119379172
SM 34:1;2	1,379044875	1,422397095	1,409906841	1,508314517	1,827266062	2,339429547	1,698557588	1,554607053	1,116922225	1,010435181	0,88598839	1,544133278	1,055109623	1,036874096	1,537368368	1,633305104	1,766554906	1,573531815	1,322267816	1,331204909	1,402075392	1,370203113	1,59289892	1,549552099	1,479291276	1,528315479	1,498526735	1,596534842
SM 34:2;2	0,136331274	0,136197952	0,152786521	0,168115061	0,146835042	0,256426528	0,280238137	0,129121639	0,092430486	0,082204036	0,081695887	0,113080921	0,093056496	0,077043003	0,192372637	0,193297396	0,228897425	0,197553568	0,121300183	0,12291939	0,129395335	0,124627498	0,204406895	0,198349139	0,138690954	0,13960982	0,146569363	0,151529112
SM 36:0;2	0,010613342	0,003086788	0,001903896	0,003319838	0,018206936	0,006984465	0,005963345	0,020143454	0,014834003	0,011546762	0,004341148	0,023736737	0,005004268	0,010939923														
SM 36:1;2	0,111311225	0,087948282	0,104240389	0,117799662	0,147267904	0,297941891	0,161091821	0,143831033	0,115502165	0,084858761	0,068692793	0,189299085	0,106489273	0,105866042	0,126557811	0,135760367	0,140225467	0,124595708	0,105052984	0,10697464	0,087972896	0,086246042	0,158336401	0,154083614	0,159462653	0,162094831	0,120475257	0,125819209
SM 36:2;2															0,05619739	0,057080677	0,065339711	0,053891164	0,047088326	0,048609786	0,035826291	0,034097258	0,071892391	0,067285537	0,065045183	0,077420108	0,046170893	0,047969879
SM 38:1;2	0,053710757	0,046494484	0,050563347	0,0557831	0,06801766	0,12121115	0,07621836	0,067686767	0,047923674	0,038610605	0,028392865	0,083581574	0,046535483	0,049600595	0,065149362	0,073033171	0,072539987	0,066559396	0,044733307	0,045593845	0,050218437	0,045714153	0,088555006	0,086770996	0,07566312	0,07157054	0,0676185	0,071093673
SM 38:2;2	0,013791823	0,012671304	0,014805917	0,014676932	0,015474847	0,017099855	0,022676393	0,008794597	0,007102305	0,006540555	0,004706862	0,004855568		0,004871109														
SM 39:1;2	0,008631788	0,003983712	0,006707916	0,008611159	0,013912777	0,024666459	0,007787825	0,010056877	0,010375935	0,006237612	0,004355299	0,009877082	0,002471269	0,007096381														
SM 40:1;2	0,144582856	0,121072467	0,136640013	0,162990824	0,184604133	0,370648778	0,235681305	0,186974061	0,128559033	0,101570984	0,070190508	0,234911222	0,155606368	0,140304312	0,152477453	0,171807749	0,153696031	0,136424058	0,109377051	0,108165537	0,124626503	0,117917373	0,274958557	0,262497188	0,226053005	0,232156266	0,213731808	0,228296383
SM 40:2;2	0,120421388	0,111901956	0,126516342	0,131518765	0,11795437	0,233463994	0,15729751	0,118507261	0,062462595	0,058747535	0,045512406	0,09973983	0,083027526	0,073849292	0,165963188	0,173900997	0,188837569	0,166583823	0,089946338	0,08618015	0,108371456	0,10205092	0,248821762	0,23888332	0,14677169	0,144053677	0,152279165	0,166067954
SM 41:1;2	0,030375933	0,020457316	0,024122026	0,034353592	0,050020558	0,077871749	0,038302967	0,047178781	0,033913952	0,025585378	0,0172481	0,044206006	0,020555398	0,030051011	0,02621735	0,031212605	0,024921045	0,023476118	0,01753454	0,017942351	0,013975965	0,017463884	0,027837395	0,024642016	0,027792425	0,028854979	0,019999087	0,026872657
SM 41:2;2	0,045293466	0,032863779	0,040763882	0,048550596	0,067823132	0,094302198	0,049687893	0,06104747	0,036149514	0,02988659	0,02415436	0,04791314	0,022070821	0,033298092	0,053089708	0,060087756	0,060932173	0,050645909	0,029619368	0,027774139	0,028481375	0,0318949	0,060834781	0,058869238	0,042603399	0,041612269	0,040676848	0,046134064
SM 42:1;2	0,196079562	0,194692386	0,185658109	0,228332211	0,246439877	0,305990331	0,249991929	0,193299919	0,14661737	0,116297272	0,081072425	0,205478466	0,129922446	0,110338089	0,123472728	0,140543052	0,100769691	0,085589908	0,182990254	0,187348015	0,188787107	0,182706861	0,104330747	0,099504716	0,244629829	0,245738263	0,231836393	0,242945446
SM 42:2;2	0,570638826	0,590043244	0,562924032	0,614648687	0,612659313	0,853295726	0,652272681	0,5162205	0,326127505	0,280813802	0,219599694	0,422102048	0,322104789	0,288738015	0,691421825	0,752274097	0,698999355	0,616438364	0,489905664	0,486205899	0,59704259	0,563888477	0,706755261	0,68143878	0,636301849	0,64636693	0,659279417	0,714920684
SM 42:3;2	0,137258161	0,138315224	0,148776197	0,159092092	0,116526251	0,211859257	0,162096483	0,100275121	0,059138795	0,051176303	0,044155869	0,075156661	0,059775395	0,057070346	0,222679898	0,221621284	0,235621272	0,200679094	0,106533489	0,106767683	0,129747427	0,121287343	0,228551701	0,213992241	0,135522321	0,138137205	0,155980782	0,167659211
Chol	22,07218881	22,24317818	20,81294543	22,87414221	23,13936982	37,50062927	27,33486136	24,0617713	23,85992818	19,69566931	18,15199005	25,37850668	25,39298359	23,60297269	21,98982538	23,50826958	23,00863291	20,53390517	25,79685437	25,88807495	26,61766831	25,44372358	24,15774518	23,12311814	26,737739	27,76051406	28,07578716	28,83147616

Table S2. siRNA sequences, related to knockdown experiments

Gene name	SiRNA ID#	Sequence, sense 5´-3´	Seguence, antisense 5´-3´
Dgat1	111783	GCAAUGCCCGGUUAUUUCUtt	AGAAAUAACCGGGCAUUGCtc
Dgat2	112268	GCUACAGGUCAUCUCAGUGtt	GGACUGCUCACCAACUCUAtt
CTα	15618	GGCUUCACGGUGAUGAACGtt	CGUUCAUCACCGUGAAGCCtt
PEMT	43023	CCUUCAAUCCGCUCUACUGtt	CAGUAGAGCGGAUUGAAGGtg

Table S3. Primers, related to knockdown experiments

Gene name	Reverse	Forward
DGAT1	CCACCAGGATGCCATACTTG	GGATCTGAGGTGCCATCGT
DGAT2	TAGATGGGAACCAGGTCAGC	CAAAGAATGGGAGTGGCAAT
CTα	ATCTTCTTCTGTTGCCCCGT	GCGCCACCTCAGAAGATAAA
PEMT	GGAAGTTCAGGAGCAGGATG	CCTTCAATCCGCTCTACTGG
mHPRT	AATCCAGCAGGTCAGCAAAG	CATTATGCCGAGGATTTGGA
hHPRT	CAAGACATTCTTTCCAGTTAAAGTTG	TTTGCTGACCTGCTGGATTAC
***Pb*18S**	GGAGATTGGTTTTGACGTTTATGTG	AAGCATTAAATAAAGCGAATACATCCTTAC